



RICE ENGINEERING

Mechanical Engineering

Seminar Series | 2020-2021



Rambod Mojgani, PhD
Postdoctoral Fellow
Department of Mechanical Engineering
Rice University

Reduced Order Modeling of Convection-Dominated Flows, Dimensionality Reduction and Stabilization

Wednesday, October 28

Zoom Webinar: 943 9612 8475

Passcode: MECH

4:00 pm - 5:00 pm

Host: Pedram Hassanzadeh, PhD

Abstract:

In this seminar, I present methodologies for reduced order modeling of convection dominated flows. Accordingly, three main problems are addressed.

Firstly, an optimal manifold is realized to enhance reducibility of convection dominated flows. We design a physics-aware auto-encoder to specifically reduce the dimensionality of solution arising from convection-dominated nonlinear physical systems. Although existing nonlinear manifold learning methods seem to be compelling tools to reduce the dimensionality of data characterized by large Kolmogorov n-width, they typically lack a straightforward mapping from the latent space to the high-dimensional physical space. Also, considering that the latent variables are often hard to interpret, many of these methods are dismissed in the reduced order modeling of dynamical systems governed by partial differential equations (PDEs). This deficiency is of importance to the extent that linear methods, such as principal component analysis (PCA) and Koopman operators, are still prevalent. Accordingly, we propose an interpretable nonlinear dimensionality reduction algorithm. An unsupervised learning problem is constructed that learns a diffeomorphic spatio-temporal grid which registers the output sequence of the PDEs on a non-uniform time-varying grid. The Kolmogorov n-width of the mapped data on the learned grid is minimized.

Secondly, the reduced order models are constructed on the realized manifolds. We project the high-fidelity models on the learned manifold, leading to a time-varying system of equations. Moreover, as a data-driven model free architecture, recurrent neural networks on the learned manifold are trained, showing the versatility of the proposed framework.

Finally, a stabilization method is developed to maintain stability and accuracy of the projection-based ROMs on the learned manifold a posteriori. We extend the eigenvalue reassignment method of stabilization of linear time-invariant ROMs, to the more general case of linear time-varying systems. Through a post-processing step, the ROMs are controlled using a constrained nonlinear lease-square minimization problem. The controller and the input signals are defined at the algebraic level, using left and right singular vectors of the reduced system matrices. The proposed stabilization method is general and applicable to a large variety of linear time-varying ROMs.

Biography:

Dr. Rambod Mojgani is a postdoctoral fellow in the Environmental Fluid Dynamics Group at Rice University working with Dr. Hassanzadeh. He received his Ph.D. from the University of Illinois at Urbana-Champaign in 2020. His dissertation on reduced order models focuses on convection dominated fluid flows and has received the Computational Science and Engineering Fellowship of 2017 from the Grainger College of Engineering, UIUC.

Reduced Order Modeling of Convection-Dominated Flows, Dimensionality Reduction and Stabilization

Rambod Mojgani

Department of Aerospace Engineering
University of Illinois at Urbana-Champaign
Dr. Maciej Balajewicz, Director of Research

Department of Mechanical Engineering — Rice University
The Environmental Fluid Dynamics Group
Prof. Pedram Hassanzadeh

Slides on: <https://github.com/rmojgani>

October 28, 2020
MECH Seminar Series, Rice University

Outline

- 1 Introduction
 - Fundamentals
 - Motivation
- 2 Identifying an optimal manifold
 - Physics-aware registration-based manifold
- 3 ROMs on the identified manifold
 - Projection based ROMs
 - Neural Network based ROMs
- 4 Stabilization of time-varying ROMs
 - A feedback controller approach
- 5 Summary

Outline

1 Introduction

- Fundamentals
- Motivation

2 Identifying an optimal manifold

- Physics-aware registration-based manifold

3 ROMs on the identified manifold

- Projection based ROMs
- Neural Network based ROMs

4 Stabilization of time-varying ROMs

- A feedback controller approach

5 Summary

Numerical simulation of physical systems



Figure 1: From high fidelity simulations to reduced order models

- Low cost computational models are especially required in
 - In situ real-time calculations
 - Many-query applications
 - Optimization
 - Uncertainty quantification (UQ)

[1] J. Lee and T. Zaki, Gallery of Fluid Motion, APS, 2017 [2] D-G Caprare et. al., Gallery of Fluid Motion, APS, 2017 [3] M. Balajewicz, 2017.

Projection based reduced order models

→ Underlying mathematical premises:

1. **Compression:** solution of governing PDEs lies on a manifold of significantly lower dimension
2. **Off-line training:**
 - the manifold can be identified/learned off-line via training simulations
 - the high-fidelity model can be reformulated with respect to this manifold, i.e. training of reduced order models (ROMs)
3. **On-line prediction:** the identified ROMs are, in principle, capable of delivering new solutions with fraction of the computational cost

Projection based reduced order models

→ Underlying mathematical premises:

1. **Compression:** solution of governing PDEs lies on a manifold of significantly lower dimension
2. **Off-line training:**
 - the manifold can be identified/learned off-line via training simulations
 - the high-fidelity model can be reformulated with respect to this manifold, i.e. training of reduced order models (ROMs)
3. **On-line prediction:** the identified ROMs are, in principle, capable of delivering new solutions with fraction of the computational cost

Projection based reduced order models

→ Underlying mathematical premises:

1. **Compression:** solution of governing PDEs lies on a manifold of significantly lower dimension
2. **Off-line training:**
 - the manifold can be identified/learned off-line via training simulations
 - the high-fidelity model can be reformulated with respect to this manifold, i.e. training of reduced order models (ROMs)
3. **On-line prediction:** the identified ROMs are, in principle, capable of delivering new solutions with fraction of the computational cost

Projection based reduced order models

→ Underlying mathematical premises:

1. **Compression:** solution of governing PDEs lies on a manifold of significantly lower dimension
2. **Off-line training:**
 - the manifold can be identified/learned off-line via training simulations
 - the high-fidelity model can be reformulated with respect to this manifold, i.e. training of reduced order models (ROMs)
3. **On-line prediction:** the identified ROMs are, in principle, capable of delivering new solutions with fraction of the computational cost

Step 1: identifying the POD subspace

- Given a snapshot matrix, $\mathbf{M} \in \mathbb{R}^{N \times K}$

$$\mathbf{M} = [\mathbf{w}_1 \quad \mathbf{w}_2 \quad \mathbf{w}_3 \quad \cdots \quad \mathbf{w}_K]; \quad \mathbf{w}_i \in \mathbb{R}^N \quad (1)$$

- The low-rank approximation problem is

$$\underset{\text{rank}(\widetilde{\mathbf{M}})=k}{\text{minimize}} \quad \|\mathbf{M} - \widetilde{\mathbf{M}}\|_F \quad (2)$$

- The rank constraint is satisfied

$$\underset{\mathbf{U} \in \mathbb{R}^{N \times k}, \mathbf{V} \in \mathbb{R}^{k \times K}}{\text{minimize}} \quad \|\mathbf{M} - \mathbf{UV}\|_F \quad (3)$$

- The solution is given by SVD/POD of the snapshot matrix

Step 1: identifying the POD subspace

- Given a snapshot matrix, $\mathbf{M} \in \mathbb{R}^{N \times K}$

$$\mathbf{M} = [\mathbf{w}_1 \quad \mathbf{w}_2 \quad \mathbf{w}_3 \quad \cdots \quad \mathbf{w}_K]; \quad \mathbf{w}_i \in \mathbb{R}^N \quad (1)$$

- The low-rank approximation problem is

$$\underset{\text{rank}(\widetilde{\mathbf{M}})=k}{\text{minimize}} \quad \|\mathbf{M} - \widetilde{\mathbf{M}}\|_F \quad (2)$$

- The rank constraint is satisfied

$$\underset{\mathbf{U} \in \mathbb{R}^{N \times k}, \mathbf{V} \in \mathbb{R}^{k \times K}}{\text{minimize}} \quad \|\mathbf{M} - \mathbf{UV}\|_F \quad (3)$$

- The solution is given by SVD/POD of the snapshot matrix

Step 1: identifying the POD subspace

- Given a snapshot matrix, $\mathbf{M} \in \mathbb{R}^{N \times K}$

$$\mathbf{M} = [\mathbf{w}_1 \quad \mathbf{w}_2 \quad \mathbf{w}_3 \quad \cdots \quad \mathbf{w}_K]; \quad \mathbf{w}_i \in \mathbb{R}^N \quad (1)$$

- The low-rank approximation problem is

$$\underset{\text{rank}(\widetilde{\mathbf{M}})=k}{\text{minimize}} \quad \|\mathbf{M} - \widetilde{\mathbf{M}}\|_F \quad (2)$$

- The rank constraint is satisfied

$$\underset{\mathbf{U} \in \mathbb{R}^{N \times k}, \mathbf{V} \in \mathbb{R}^{k \times K}}{\text{minimize}} \quad \|\mathbf{M} - \mathbf{U}\mathbf{V}\|_F \quad (3)$$

- The solution is given by SVD/POD of the snapshot matrix

Step 1: identifying the POD subspace

- Given a snapshot matrix, $\mathbf{M} \in \mathbb{R}^{N \times K}$

$$\mathbf{M} = [\mathbf{w}_1 \quad \mathbf{w}_2 \quad \mathbf{w}_3 \quad \cdots \quad \mathbf{w}_K]; \quad \mathbf{w}_i \in \mathbb{R}^N \quad (1)$$

- The low-rank approximation problem is

$$\underset{\text{rank}(\widetilde{\mathbf{M}})=k}{\text{minimize}} \quad \|\mathbf{M} - \widetilde{\mathbf{M}}\|_F \quad (2)$$

- The rank constraint is satisfied

$$\underset{\mathbf{U} \in \mathbb{R}^{N \times k}, \mathbf{V} \in \mathbb{R}^{k \times K}}{\text{minimize}} \quad \|\mathbf{M} - \mathbf{U}\mathbf{V}\|_F \quad (3)$$

- The solution is given by SVD/POD of the snapshot matrix

Step 2: constructing the reduced order model

- Consider the discretized system

$$\mathbf{R}(\mathbf{w}[n]) = \mathbf{0} \quad (4)$$

- The state, \mathbf{w} , is approximated on a global trial subspace,

$$\mathbf{w}[n] \approx \tilde{\mathbf{w}}[n] = \mathbf{U}\mathbf{w}_r[n], \quad \mathbf{U} \in \mathbb{R}^{N \times k}, \quad \mathbf{w}_r[n] \in \mathbb{R}^k, \quad k \ll N \quad (5)$$

- Galerkin projection onto the test subspace $\mathbf{U} \in \mathbb{R}^{N \times k}$,

$$\mathbf{U}^T \mathbf{R}(\mathbf{U}\mathbf{w}_r[n]) = \mathbf{0} \quad (6)$$

Step 2: constructing the reduced order model

- Consider the discretized system

$$\mathbf{R}(\mathbf{w}[n]) = \mathbf{0} \quad (4)$$

- The state, \mathbf{w} , is approximated on a global trial subspace,

$$\mathbf{w}[n] \approx \tilde{\mathbf{w}}[n] = \mathbf{U}\mathbf{w}_r[n], \quad \mathbf{U} \in \mathbb{R}^{N \times k}, \quad \mathbf{w}_r[n] \in \mathbb{R}^k, \quad k \ll N \quad (5)$$

- Galerkin projection onto the test subspace $\mathbf{U} \in \mathbb{R}^{N \times k}$,

$$\mathbf{U}^T \mathbf{R}(\mathbf{U}\mathbf{w}_r[n]) = \mathbf{0} \quad (6)$$

Step 2: constructing the reduced order model

- Consider the discretized system

$$\mathbf{R}(\mathbf{w}[n]) = \mathbf{0} \quad (4)$$

- The state, \mathbf{w} , is approximated on a global trial subspace,

$$\mathbf{w}[n] \approx \tilde{\mathbf{w}}[n] = \mathbf{U}\mathbf{w}_r[n], \quad \mathbf{U} \in \mathbb{R}^{N \times k}, \quad \mathbf{w}_r[n] \in \mathbb{R}^k, \quad k \ll N \quad (5)$$

- Galerkin projection onto the test subspace $\mathbf{U} \in \mathbb{R}^{N \times k}$,

$$\mathbf{U}^T \mathbf{R}(\mathbf{U}\mathbf{w}_r[n]) = \mathbf{0} \quad (6)$$

Motivational problem 1: one-dimensional convection

- Consider the scalar linear convection equation

$$\begin{cases} \frac{\partial w}{\partial t} + \frac{\partial w}{\partial x} = 0, & (x, t) \in [0, \infty) \times [0, 1] \\ w(x, 0) = 0.8 + e^{-(x-0.3)^2/0.05^2} \\ w(0, t) = 0.8 \end{cases} \quad (7)$$

- Exact solution is $w(x, t) = w(x - t, 0)$

Motivational problem 1: one-dimensional convection

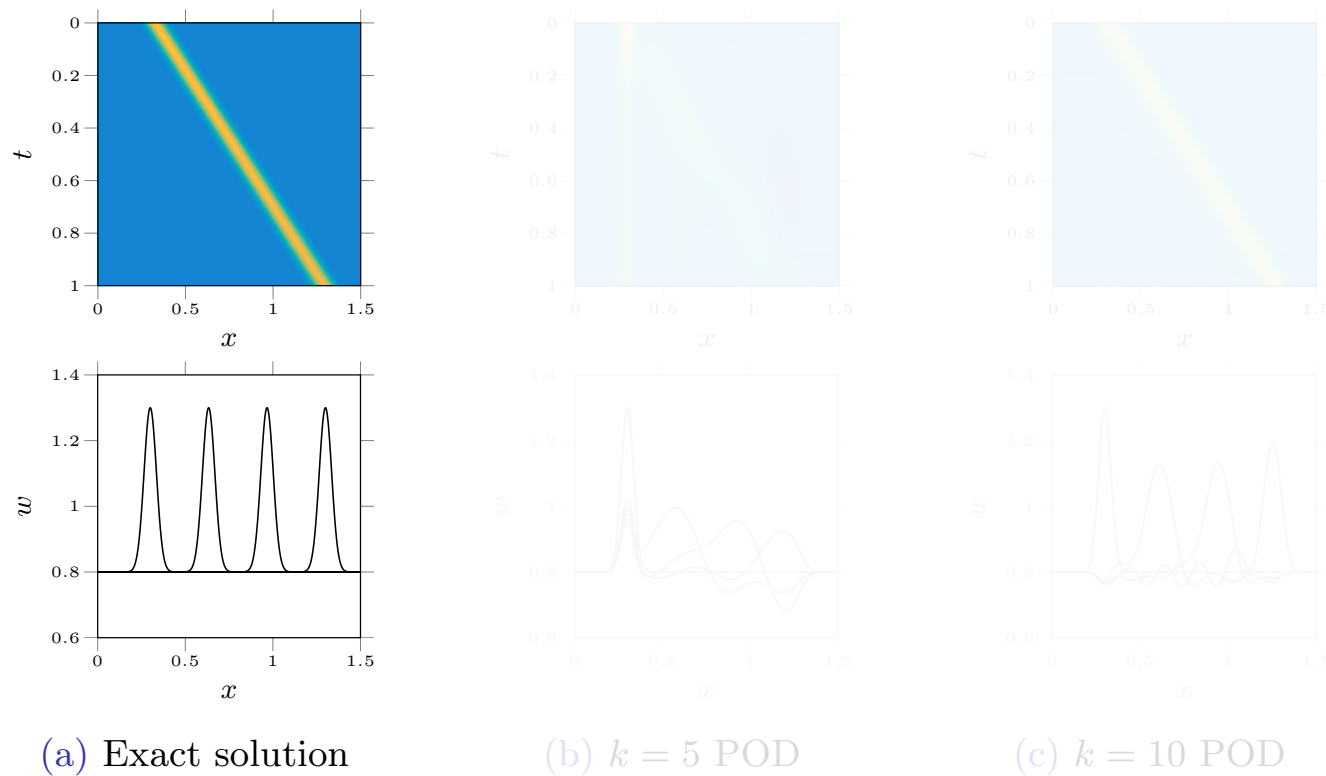


Figure 2: POD compression of the scalar convection equation

Motivational problem 1: one-dimensional convection

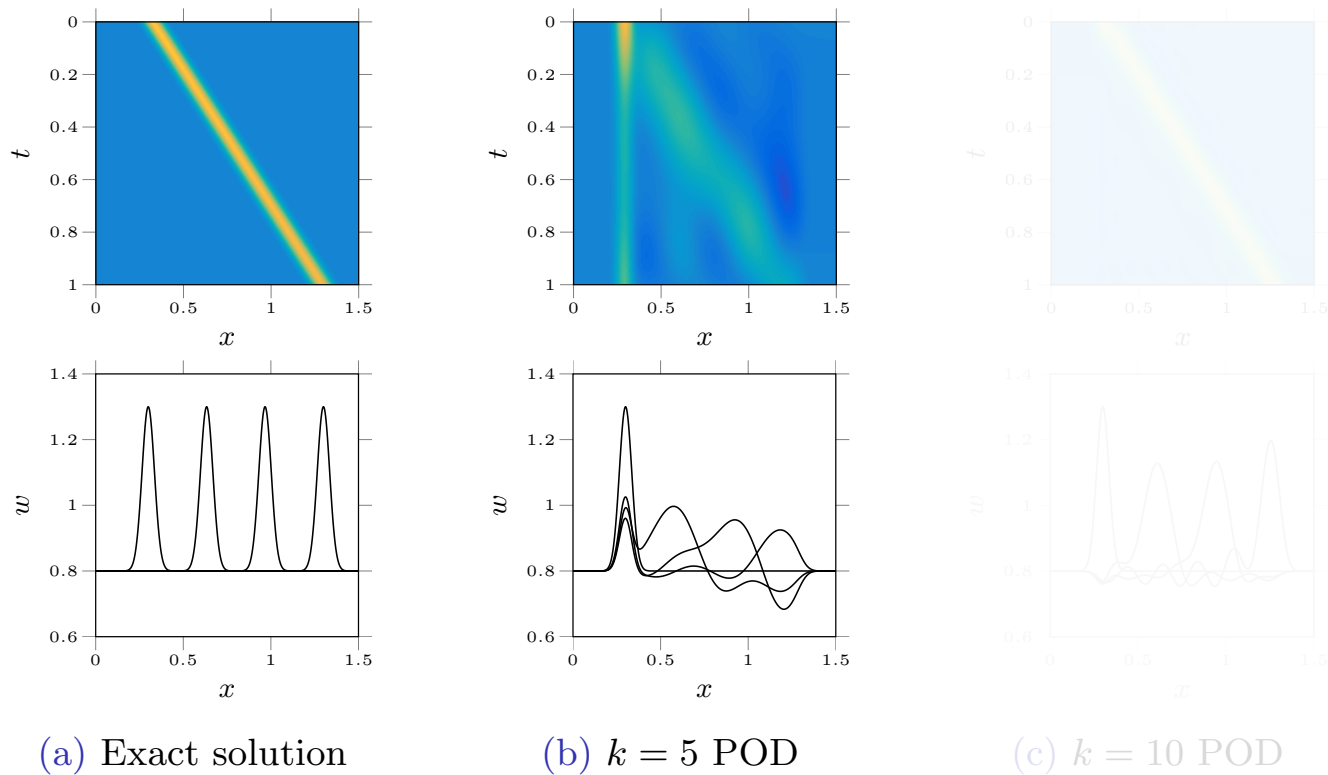


Figure 2: POD compression of the scalar convection equation

Motivational problem 1: one-dimensional convection

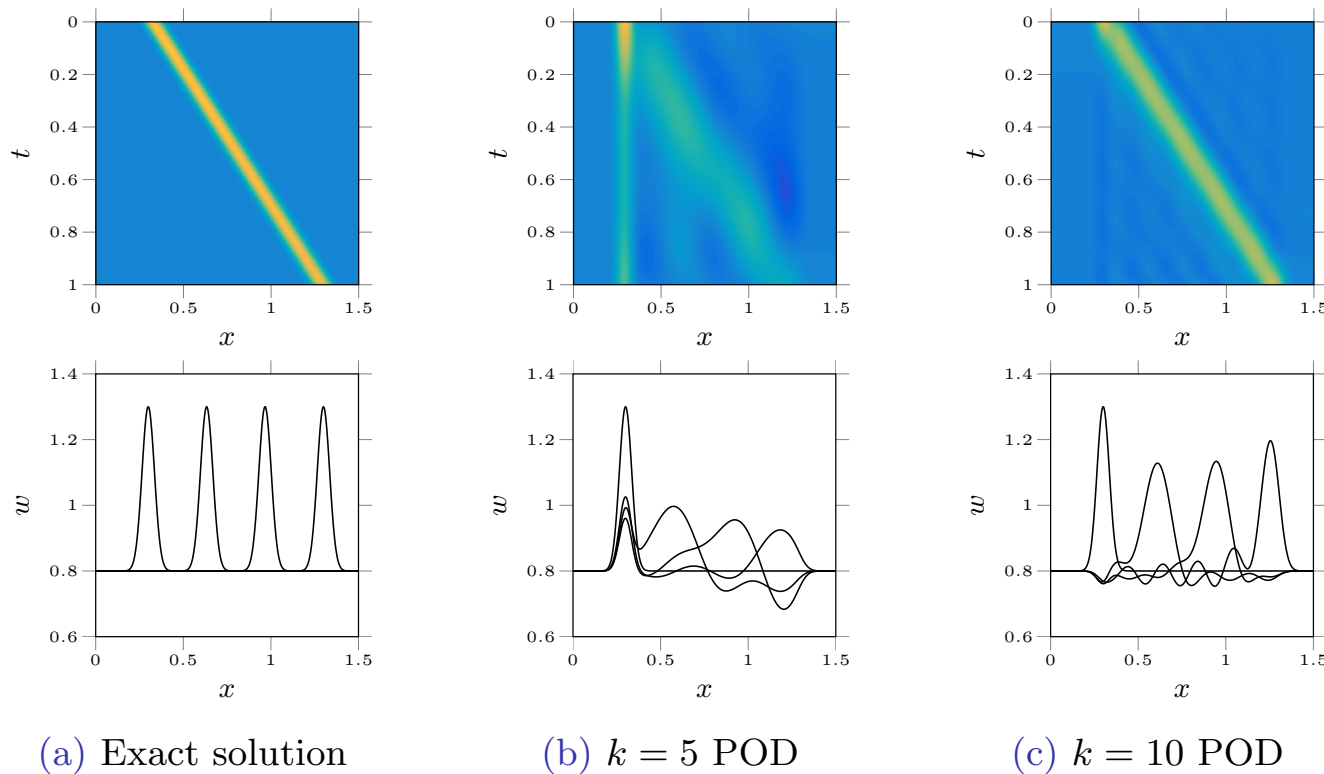


Figure 2: POD compression of the scalar convection equation

Motivational problem 2: Rotating character “A”

- Each snapshot is a 50×50 matrix of real numbers corresponding to greyscale values of the character “A”

A A A A A A A A A

(a) The snapshots



(b) The rank-1 reconstruction ($k = 1$) on the POD subspace

Figure 3: POD compression of 90 degrees rotation of character “A”

Motivational problem 2: Rotating character “A”

- Each snapshot is a 50×50 matrix of real numbers corresponding to greyscale values of the character “A”

A A A A A A A A A

(a) The snapshots



(b) The rank-1 reconstruction ($k = 1$) on the POD subspace

Figure 3: POD compression of 90 degrees rotation of character “A”

Motivation: observations

- Despite relative simplicity of the snapshots, these particular two examples could not be approximated using a *small* number of bases using the traditional *linear* approach
- It is simply not possible to efficiently compress certain wave-like solutions using a low-rank decomposition
- A *fundamentally* different approach is required

Motivation: observations

- Despite relative simplicity of the snapshots, these particular two examples could not be approximated using a *small* number of bases using the traditional *linear* approach
- It is simply not possible to efficiently compress certain wave-like solutions using a low-rank decomposition
- A *fundamentally* different approach is required

Motivation: observations

- Despite relative simplicity of the snapshots, these particular two examples could not be approximated using a *small* number of bases using the traditional *linear* approach
- It is simply not possible to efficiently compress certain wave-like solutions using a low-rank decomposition
- A *fundamentally* different approach is required

Previous attempts

1. Seeking symmetries, self-similarities, and coordinate transformations or modifying the decomposition to include the mentioned properties, i.e. \mathcal{L} -DMD, sPOD
[Rowley and Marsden, 2000, Rowley et al., 2003, Kavousanakis et al., 2007, Rapun and Vega, 2010, Gerbeau and Lombardi, 2014, Rim et al., 2017, Mowlavi and Sapsis, 2018, Rim and Mandli, 2018, Reiss et al., 2015, Reiss et al., 2018, Schulze et al., 2018, Mendible et al., 2019, Taddei, 2020]
2. Using local bases or splitting the domain or bases
[Amsallem et al., 2012, Lucia, 2001, Carlberg, 2015]
3. Adding temporal dependency in the reduced bases
[Iollo and Lombardi, 2014, Gerbeau and Lombardi, 2014, Babaee et al., 2017].

Previous attempts

1. Seeking symmetries, self-similarities, and coordinate transformations or modifying the decomposition to include the mentioned properties, i.e. \mathcal{L} -DMD, sPOD
[Rowley and Marsden, 2000, Rowley et al., 2003, Kavousanakis et al., 2007, Rapun and Vega, 2010, Gerbeau and Lombardi, 2014, Rim et al., 2017, Mowlavi and Sapsis, 2018, Rim and Mandli, 2018, Reiss et al., 2015, Reiss et al., 2018, Schulze et al., 2018, Mendible et al., 2019, Taddei, 2020]
2. Using local bases or splitting the domain or bases
[Amsallem et al., 2012, Lucia, 2001, Carlberg, 2015]
3. Adding temporal dependency in the reduced bases
[Iollo and Lombardi, 2014, Gerbeau and Lombardi, 2014, Babaee et al., 2017].

Previous attempts

1. Seeking symmetries, self-similarities, and coordinate transformations or modifying the decomposition to include the mentioned properties, i.e. \mathcal{L} -DMD, sPOD
[Rowley and Marsden, 2000, Rowley et al., 2003, Kavousanakis et al., 2007, Rapun and Vega, 2010, Gerbeau and Lombardi, 2014, Rim et al., 2017, Mowlavi and Sapsis, 2018, Rim and Mandli, 2018, Reiss et al., 2015, Reiss et al., 2018, Schulze et al., 2018, Mendible et al., 2019, Taddei, 2020]
2. Using local bases or splitting the domain or bases
[Amsallem et al., 2012, Lucia, 2001, Carlberg, 2015]
3. Adding temporal dependency in the reduced bases
[Iollo and Lombardi, 2014, Gerbeau and Lombardi, 2014, Babaee et al., 2017].

Identifying a subspace/manifold

- We propose to construct the ROMs on *nonlinear* manifolds
- Linear subspaces
 - Proper Orthogonal Decomposition (POD)
 - Dynamic Mode Decomposition (DMD)
 - ...
- Nonlinear manifolds
 - Iso-map [Tenenbaum, 1998]
 - t-distributed stochastic neighbor embedding (t-SNE) [Maaten and Hinton, 2008]
 - Auto-encoders [G.E and R.R, 2006]
 - ...
- The goals of the proposed approach
 - Data-driven
 - Compressibility on the identified manifold
 - A two-way map between the physical space and latent space
 - Interpretable low-dimensional/latent variables

Identifying a subspace/manifold

- We propose to construct the ROMs on *nonlinear* manifolds
- Linear subspaces
 - Proper Orthogonal Decomposition (POD)
 - Dynamic Mode Decomposition (DMD)
 - ...
- Nonlinear manifolds
 - Iso-map [Tenenbaum, 1998]
 - t-distributed stochastic neighbor embedding (t-SNE) [Maaten and Hinton, 2008]
 - Auto-encoders [G.E and R.R, 2006]
 - ...
- The goals of the proposed approach
 - Data-driven
 - Compressibility on the identified manifold
 - A two-way map between the physical space and latent space
 - Interpretable low-dimensional/latent variables

Identifying a subspace/manifold

- We propose to construct the ROMs on *nonlinear* manifolds
- Linear subspaces
 - Proper Orthogonal Decomposition (POD)
 - Dynamic Mode Decomposition (DMD)
 - ...
- Nonlinear manifolds
 - Iso-map [Tenenbaum, 1998]
 - t-distributed stochastic neighbor embedding (t-SNE) [Maaten and Hinton, 2008]
 - Auto-encoders [G.E and R.R, 2006]
 - ...
- The goals of the proposed approach
 - Data-driven
 - Compressibility on the identified manifold
 - A two-way map between the physical space and latent space
 - Interpretable low-dimensional/latent variables

Identifying a subspace/manifold

- We propose to construct the ROMs on *nonlinear* manifolds
- Linear subspaces
 - Proper Orthogonal Decomposition (POD)
 - Dynamic Mode Decomposition (DMD)
 - ...
- Nonlinear manifolds
 - Iso-map [Tenenbaum, 1998]
 - t-distributed stochastic neighbor embedding (t-SNE) [Maaten and Hinton, 2008]
 - Auto-encoders [G.E and R.R, 2006]
 - ...
- The goals of the proposed approach
 - Data-driven
 - Compressibility on the identified manifold
 - A two-way map between the physical space and latent space
 - Interpretable low-dimensional/latent variables

Outline

1 Introduction

- Fundamentals
- Motivation

2 Identifying an optimal manifold

- Physics-aware registration-based manifold

3 ROMs on the identified manifold

- Projection based ROMs
- Neural Network based ROMs

4 Stabilization of time-varying ROMs

- A feedback controller approach

5 Summary

The proposed manifold

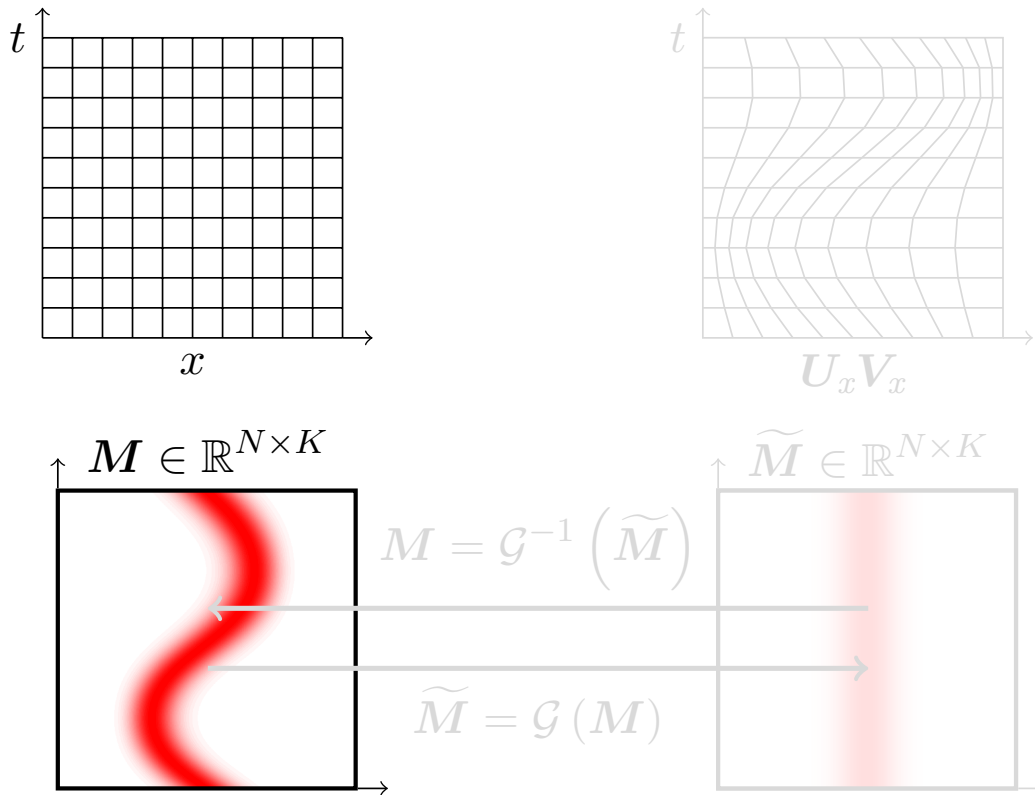


Figure 4: Illustration of the proposed approach

The proposed manifold

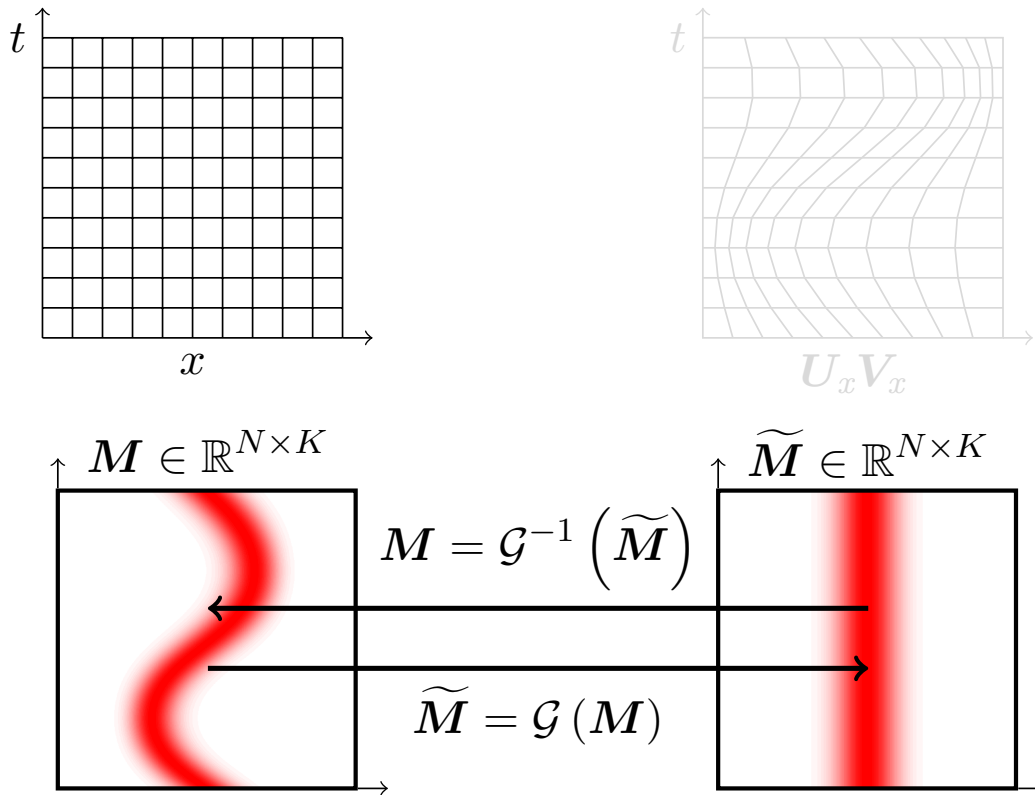


Figure 4: Illustration of the proposed approach

The proposed manifold

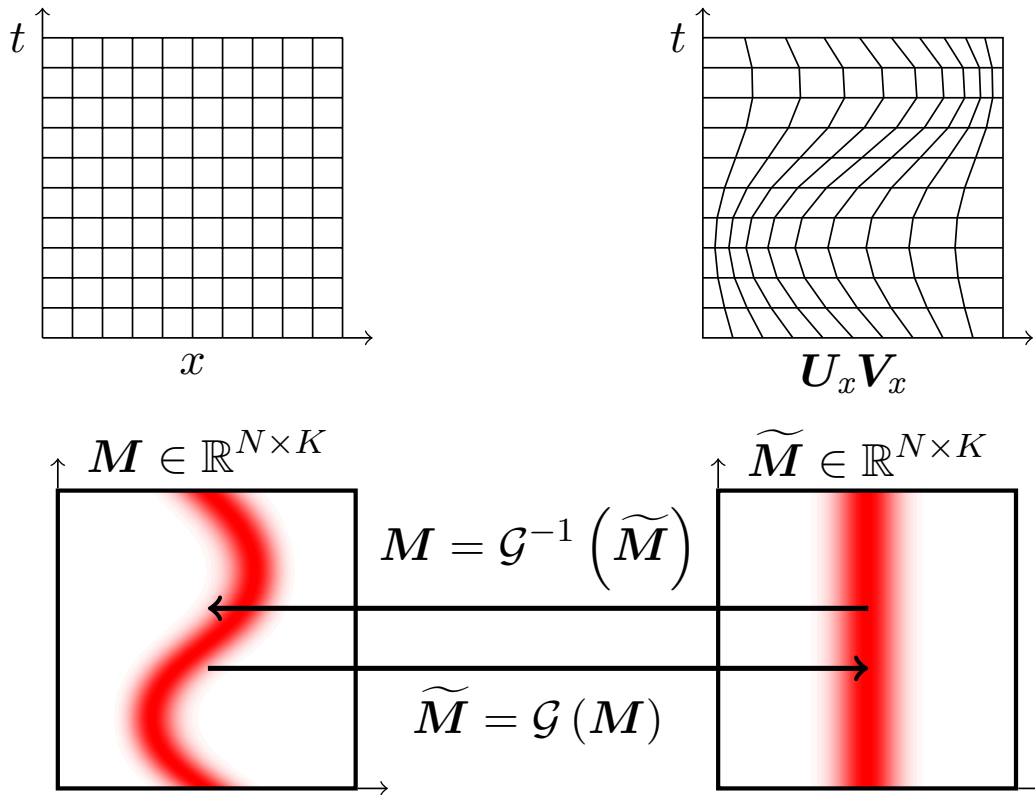


Figure 4: Illustration of the proposed approach

The proposed manifold

- For a given snapshot matrix $\mathbf{M} \in \mathbb{R}^{N \times K}$, find an empirical *map* that solves the minimization problem:

$$\underset{\mathcal{G}}{\text{minimize}} \left\| \mathbf{M} - \mathcal{G}^{-1} \left(\widetilde{\mathbf{M}} \right) \right\|_F \quad (8)$$

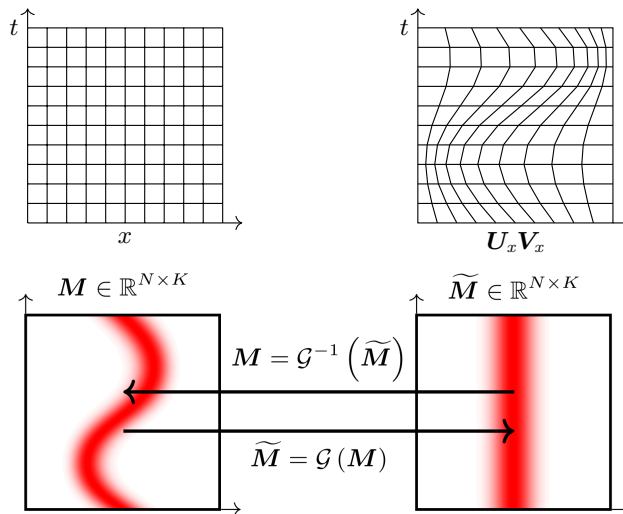


Figure 4: Illustration of the proposed approach

The proposed manifold

- For a given snapshot matrix $\mathbf{M} \in \mathbb{R}^{N \times K}$, find an empirical map that solves *low-rank approximation* problem:

$$\underset{\mathcal{G}}{\text{minimize}} \|\mathbf{M} - \mathcal{G}^{-1}(\mathbf{U}\mathbf{V})\|_F \quad (9)$$

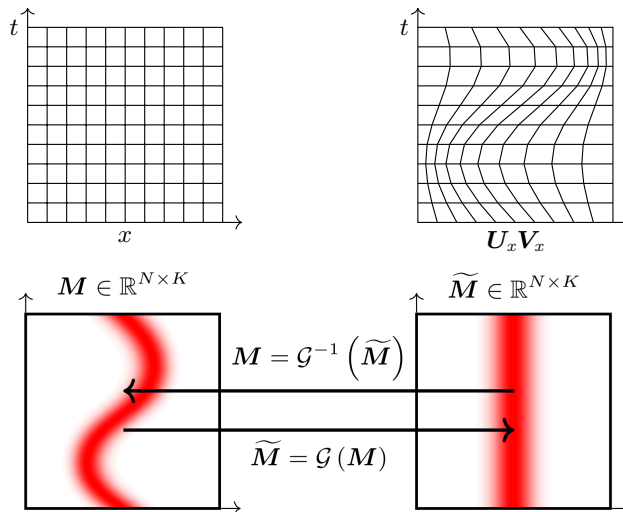


Figure 4: Illustration of the proposed approach

The proposed manifold

- For a given snapshot matrix $\mathbf{M} \in \mathbb{R}^{N \times K}$, find a *low-rank grid* that solves the minimization problem:

$$\underset{\mathbf{U}_x \in \mathbb{R}^{N \times r}, \mathbf{V}_x \in \mathbb{R}^{r \times K}}{\text{minimize}} \left\| \mathbf{M} - \mathcal{G}^{-1} (\mathbf{U} \mathbf{V}) \right\|_F \quad (10)$$

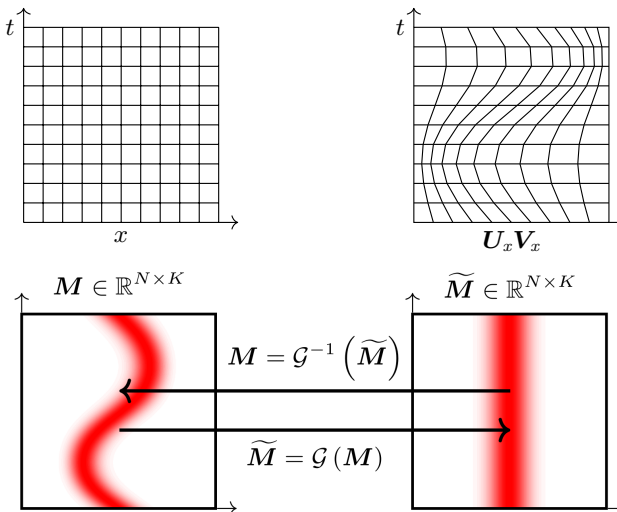


Figure 4: Illustration of the proposed approach

Interpolation and diffeomorphism

- Impose diffeomorphism: “a map, \mathcal{G} , is said to be diffeomorphic if \mathcal{G} and \mathcal{G}^{-1} are differentiable”
- Guarantees existence and uniqueness of $\widetilde{\mathbf{M}}$, given a \mathbf{M} and vice versa
- For the map to be diffeomorphic
 - Bijectivity (i.e. one to oneness)
 - Continuity of the function and its inverse function
 - Smoothness

Interpolation and diffeomorphism

- Impose diffeomorphism: “a map, \mathcal{G} , is said to be diffeomorphic if \mathcal{G} and \mathcal{G}^{-1} are differentiable”
- Guarantees existence and uniqueness of $\widetilde{\mathbf{M}}$, given a \mathbf{M} and vice versa
- For the map to be diffeomorphic
 - Bijectivity (i.e. one to oneness)
 - Continuity
 - Smoothness

Interpolation and diffeomorphism

- Impose diffeomorphism: “a map, \mathcal{G} , is said to be diffeomorphic if \mathcal{G} and \mathcal{G}^{-1} are differentiable”
- Guarantees existence and uniqueness of $\widetilde{\mathbf{M}}$, given a \mathbf{M} and vice versa
- For the map to be diffeomorphic
 - Bijectivity (i.e. one to oneness)
 - is enforced by ensuring that volume of all the cells remain strictly positive
 - Smoothness
 - is promoted by penalizing abrupt changes of the grid volume, both in space and parameter/time

Interpolation and diffeomorphism

- Impose diffeomorphism: “a map, \mathcal{G} , is said to be diffeomorphic if \mathcal{G} and \mathcal{G}^{-1} are differentiable”
- Guarantees existence and uniqueness of $\widetilde{\mathbf{M}}$, given a \mathbf{M} and vice versa
- For the map to be diffeomorphic
 - Bijectivity (i.e. one to oneness)
 - is enforced by ensuring that volume of all the cells remain strictly positive
 - Smoothness
 - is promoted by penalizing abrupt changes of the grid volume, both in space and parameter/time

Physics-aware registration based auto-encoder

- The final minimization problem:

$$\begin{aligned}
 & \underset{\mathbf{U}_x, \mathbf{V}_x}{\text{minimize}} \quad \|\mathbf{M} - \mathcal{G}^{-1}(\mathbf{U}\mathbf{V})\|_F + \|\boldsymbol{\Gamma}_1 \mathbf{U}_x\|_F + \|\mathbf{V}_x \boldsymbol{\Gamma}_2^T\|_F \\
 & \text{subject to } \mathbf{v}[n] \geq v_{\min}, \text{ for } n = 1, \dots, K \\
 & \quad \mathbf{x}[n]|_{\partial\Omega} = \mathbf{x}|_{\partial\Omega}, \text{ for } n = 1, \dots, K
 \end{aligned} \tag{11}$$

- $\mathbf{U} \in \mathbb{R}^{N \times k_r}$, $\mathbf{V} \in \mathbb{R}^{k_r \times K}$
- $\mathbf{U}_x \in \mathbb{R}^{N \times r}$, $\mathbf{V}_x \in \mathbb{R}^{r \times K}$
- $\boldsymbol{\Gamma}_1 \in \mathbb{R}^{N \times N}$, $\boldsymbol{\Gamma}_2 \in \mathbb{R}^{K \times K}$
- $\mathbf{v}[n] \in \mathbb{R}^N$ is a vector of cell volumes of the time-varying grid
- $\mathbf{x}[n]|_{\partial\Omega}$ and $\mathbf{x}|_{\partial\Omega}$ are boundary points of the time-varying and Eulerian grids

Physics-aware registration based auto-encoder

- The final minimization problem:

$$\begin{aligned}
 & \underset{\mathbf{U}_x, \mathbf{V}_x}{\text{minimize}} \quad \|\mathbf{M} - \mathcal{G}^{-1}(\mathbf{U}\mathbf{V})\|_F + \|\boldsymbol{\Gamma}_1 \mathbf{U}_x\|_F + \|\mathbf{V}_x \boldsymbol{\Gamma}_2^T\|_F \\
 & \text{subject to } \mathbf{v}[n] \geq v_{\min}, \text{ for } n = 1, \dots, K \\
 & \quad \mathbf{x}[n]|_{\partial\Omega} = \mathbf{x}|_{\partial\Omega}, \text{ for } n = 1, \dots, K
 \end{aligned} \tag{11}$$

- $\mathbf{U} \in \mathbb{R}^{N \times k_r}$, $\mathbf{V} \in \mathbb{R}^{k_r \times K}$
- $\mathbf{U}_x \in \mathbb{R}^{N \times r}$, $\mathbf{V}_x \in \mathbb{R}^{r \times K}$
- $\boldsymbol{\Gamma}_1 \in \mathbb{R}^{N \times N}$, $\boldsymbol{\Gamma}_2 \in \mathbb{R}^{K \times K}$
- $\mathbf{v}[n] \in \mathbb{R}^N$ is a vector of cell volumes of the time-varying grid
- $\mathbf{x}[n]|_{\partial\Omega}$ and $\mathbf{x}|_{\partial\Omega}$ are boundary points of the time-varying and Eulerian grids

Physics-aware registration based auto-encoder

- The final minimization problem:

$$\begin{aligned}
 & \underset{\mathbf{U}_x, \mathbf{V}_x}{\text{minimize}} \quad \|\mathbf{M} - \mathcal{G}^{-1}(\mathbf{U}\mathbf{V})\|_F + \|\boldsymbol{\Gamma}_1 \mathbf{U}_x\|_F + \|\mathbf{V}_x \boldsymbol{\Gamma}_2^T\|_F \\
 & \text{subject to } \mathbf{v}[n] \geq v_{\min}, \text{ for } n = 1, \dots, K \\
 & \quad \mathbf{x}[n]|_{\partial\Omega} = \mathbf{x}|_{\partial\Omega}, \text{ for } n = 1, \dots, K
 \end{aligned} \tag{11}$$

- $\mathbf{U} \in \mathbb{R}^{N \times k_r}$, $\mathbf{V} \in \mathbb{R}^{k_r \times K}$
- $\mathbf{U}_x \in \mathbb{R}^{N \times r}$, $\mathbf{V}_x \in \mathbb{R}^{r \times K}$
- $\boldsymbol{\Gamma}_1 \in \mathbb{R}^{N \times N}$, $\boldsymbol{\Gamma}_2 \in \mathbb{R}^{K \times K}$
- $\mathbf{v}[n] \in \mathbb{R}^N$ is a vector of cell volumes of the time-varying grid
- $\mathbf{x}[n]|_{\partial\Omega}$ and $\mathbf{x}|_{\partial\Omega}$ are boundary points of the time-varying and Eulerian grids

Physics-aware registration based auto-encoder

- The final minimization problem:

$$\begin{aligned}
 & \underset{\mathbf{U}_x, \mathbf{V}_x}{\text{minimize}} \quad \|\mathbf{M} - \mathcal{G}^{-1}(\mathbf{U}\mathbf{V})\|_F + \|\boldsymbol{\Gamma}_1 \mathbf{U}_x\|_F + \|\mathbf{V}_x \boldsymbol{\Gamma}_2^T\|_F \\
 & \text{subject to } \mathbf{v}[n] \geq v_{\min}, \text{ for } n = 1, \dots, K \\
 & \quad \mathbf{x}[n]|_{\partial\Omega} = \mathbf{x}|_{\partial\Omega}, \text{ for } n = 1, \dots, K
 \end{aligned} \tag{11}$$

- $\mathbf{U} \in \mathbb{R}^{N \times k_r}$, $\mathbf{V} \in \mathbb{R}^{k_r \times K}$
- $\mathbf{U}_x \in \mathbb{R}^{N \times r}$, $\mathbf{V}_x \in \mathbb{R}^{r \times K}$
- $\boldsymbol{\Gamma}_1 \in \mathbb{R}^{N \times N}$, $\boldsymbol{\Gamma}_2 \in \mathbb{R}^{K \times K}$
- $\mathbf{v}[n] \in \mathbb{R}^N$ is a vector of cell volumes of the time-varying grid
- $\mathbf{x}[n]|_{\partial\Omega}$ and $\mathbf{x}|_{\partial\Omega}$ are boundary points of the time-varying and Eulerian grids

Numerical Example: Rotating character “A”

- Each snapshot is a 50×50 matrix of real numbers corresponding to greyscale values of the character A

A A A A A A A A A

(a) The snapshots



(b) The rank-1 reconstruction ($k = 1$) on the POD subspace



(c) The rank-1 grid corresponding to the identified manifold

A A A A A A A A A

(d) The rank-1 reconstruction ($k_r = 1$) on the rank-1 grid ($r = 1$)

Figure 5: 90 degrees rotation of character “A”

Numerical Example: Rotating character “A”

- Each snapshot is a 50×50 matrix of real numbers corresponding to greyscale values of the character A

A A A A A A A A A

(a) The snapshots



(b) The rank-1 reconstruction ($k = 1$) on the POD subspace



(c) The rank-1 grid corresponding to the identified manifold

A A A A A A A A A

(d) The rank-1 reconstruction ($k_r = 1$) on the rank-1 grid ($r = 1$)

Figure 5: 90 degrees rotation of character “A”

Numerical Example: Rotating character “A”

- Each snapshot is a 50×50 matrix of real numbers corresponding to greyscale values of the character A

A A A ↗ ↗ ↗ ↗ ↗ ↗ ↗ ↗ ↗

(a) The snapshots



(b) The rank-1 reconstruction ($k = 1$) on the POD subspace



(c) The rank-1 grid corresponding to the identified manifold



(d) The rank-1 reconstruction ($k_r = 1$) on the rank-1 grid ($r = 1$)

Figure 5: 90 degrees rotation of character “A”

Numerical Example: Rotating character “A”

- Each snapshot is a 50×50 matrix of real numbers corresponding to greyscale values of the character A

A A A A A A A A A

(a) The snapshots



(b) The rank-1 reconstruction ($k = 1$) on the POD subspace



(c) The rank-1 grid corresponding to the identified manifold

A A A A A A A A A

(d) The rank-1 reconstruction ($k_r = 1$) on the rank-1 grid ($r = 1$)

Figure 5: 90 degrees rotation of character “A”

Numerical Example: Rotating character “A”

- Each snapshot is a 50×50 matrix of real numbers corresponding to greyscale values of the character A

A A A A A A A A A

(a) The snapshots



(b) The rank-1 reconstruction ($k = 1$) on the POD subspace



(c) The rank-2 grid corresponding to the identified manifold

A A A A A A A A A

(d) The rank-1 reconstruction ($k_r = 1$) on the rank-2 grid ($r = 2$)

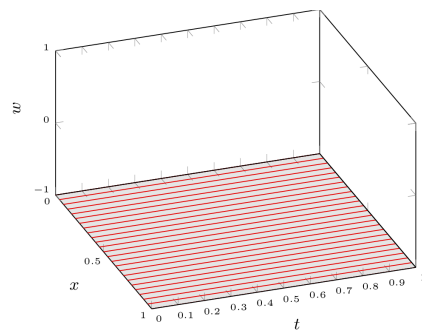
Figure 5: 90 degrees rotation of character “A”

Numerical Example: Second-order wave equation

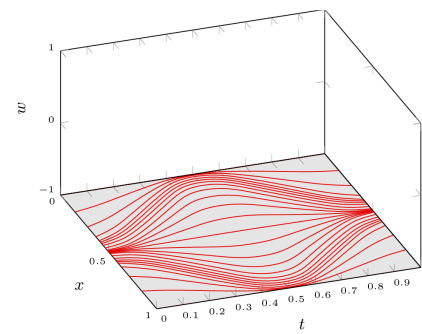
- Consider the second-order wave equation

$$\begin{cases} \frac{\partial^2 w(x, t)}{\partial t^2} - \frac{\partial^2 w(x, t)}{\partial x^2} = 0, & (x, t) \in [0, 1] \times [0, 1] \\ w(x, 0) = e^{-((x-0.5)/0.05)^2} \\ \partial_t w(x, 0) = 0 \\ w(0, t) = 0 \\ w(1, t) = 0 \end{cases} \quad (12)$$

Numerical Example: Second-order wave equation



(a) Eulerian grid



(b) Rank-2 grid

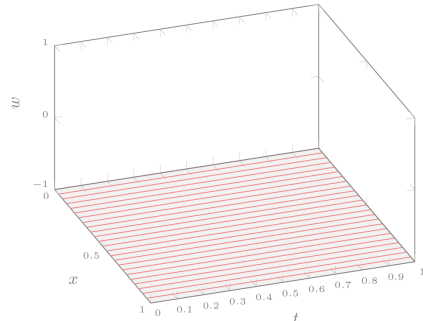
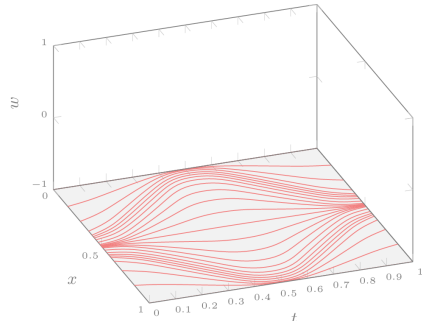
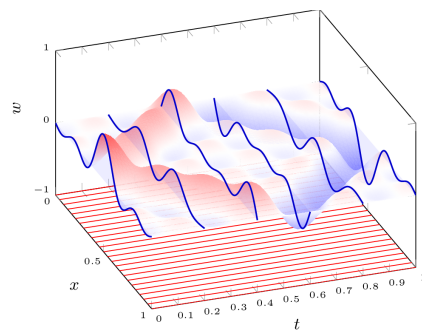
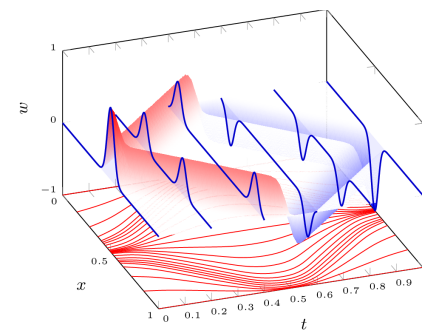
(c) Eulerian grid, $k = 8$ POD(d) Rank-2 grid, $k_r = 8$

Figure 6: Reconstruction of second-order wave equation

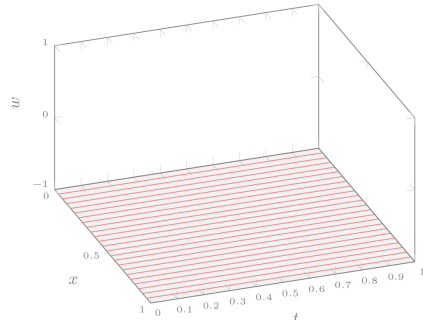
Numerical Example: Second-order wave equation



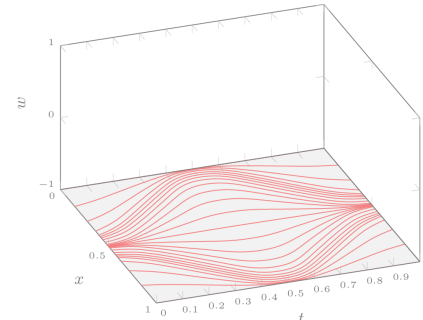
(a) Eulerian grid, $k = 4$ POD



(b) Rank-2 grid, $k_r = 4$



(c) Eulerian grid, $k = 8$ POD



(d) Rank-2 grid, $k_r = 8$

Figure 6: Reconstruction of second-order wave equation

Numerical Example: Second-order wave equation

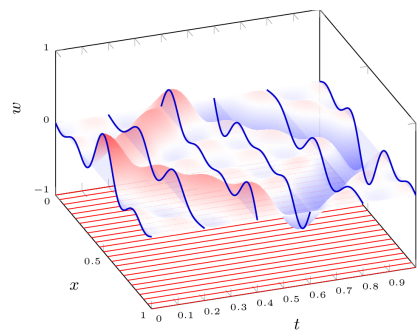
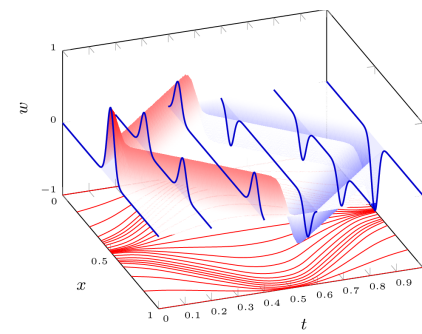
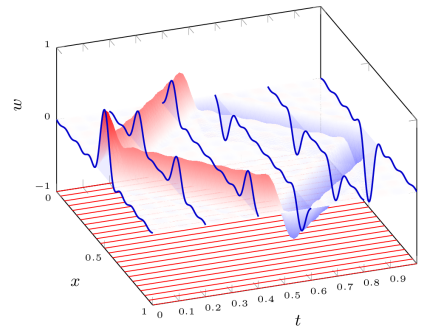
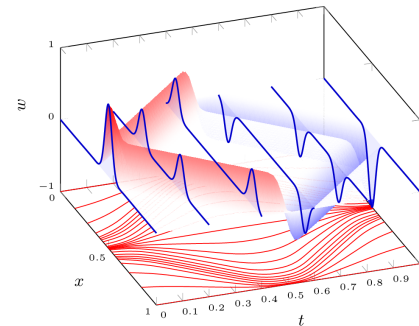
(a) Eulerian grid, $k = 4$ POD(b) Rank-2 grid, $k_r = 4$ (c) Eulerian grid, $k = 8$ POD(d) Rank-2 grid, $k_r = 8$

Figure 6: Reconstruction of second-order wave equation

Numerical Example: Second-order wave equation

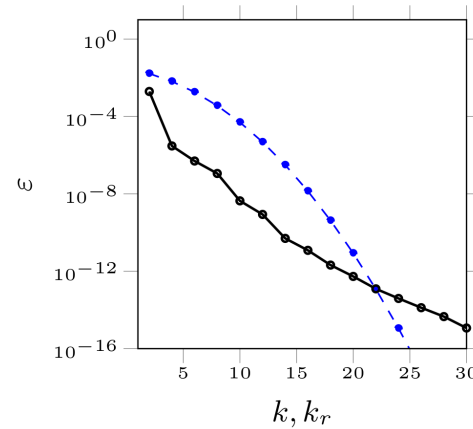


Figure 7: Reconstruction error in second-order wave problem. The rank- k reconstruction on traditional POD subspace (dashed blue line), and rank- k_r reconstruction on the identified manifold of rank-2 grid (solid black line)

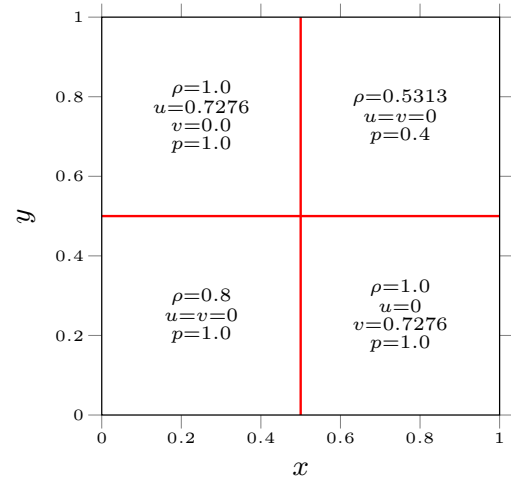
Numerical Example: Two-dimensional Riemann problem

- Consider the Euler equations

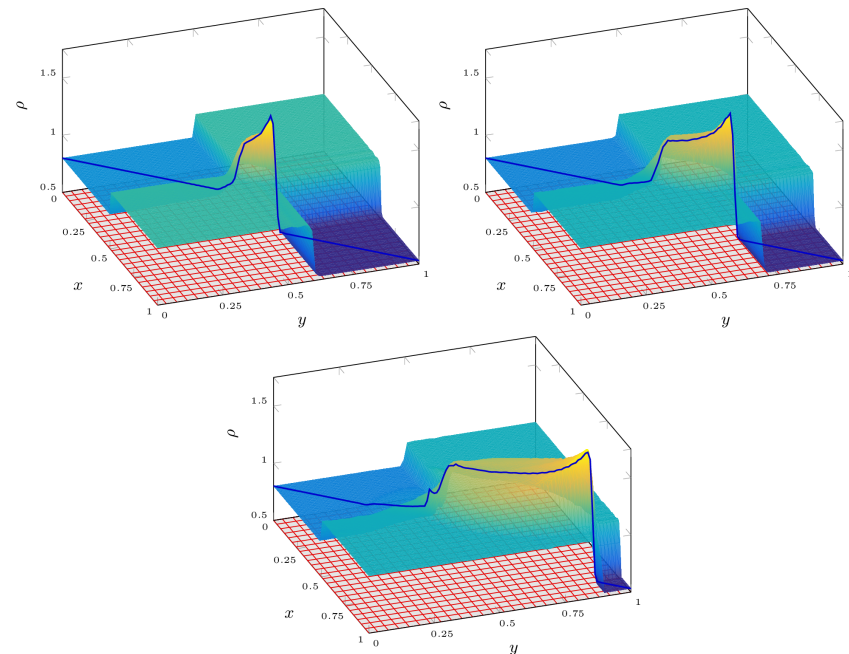
$$\left\{ \begin{array}{lcl} \frac{\partial}{\partial t} \mathbf{q} + \frac{\partial}{\partial x} \mathbf{f}_x + \frac{\partial}{\partial y} \mathbf{f}_y & = & 0, \quad (x, y, t) \in [0, 1] \times [0, 1] \times [0, t_{\max}] \\ \mathbf{q} & = & [\rho, \rho u, \rho v, \rho e]^T \\ \mathbf{f}_x & = & [\rho u, \rho u^2 + p, \rho uv, \rho uH]^T \\ \mathbf{f}_y & = & [\rho v, \rho uv + p, \rho v^2 + p, \rho vH]^T \\ H & = & e + p/\rho \\ p & = & \rho (\gamma - 1) (e - 0.5 (u^2 + v^2)) \end{array} \right. \quad (13)$$

- Stabilized using high-order artificial viscosity

Two-dimensional Riemann problem



(a) Initial condition,
configuration 12
[Lax and Liu, 1998]



(b) Density at $t \in \{0.0625, 0.125, 0.25\}$

Figure 8: Two-dimensional Riemann problem

Two-dimensional Riemann problem

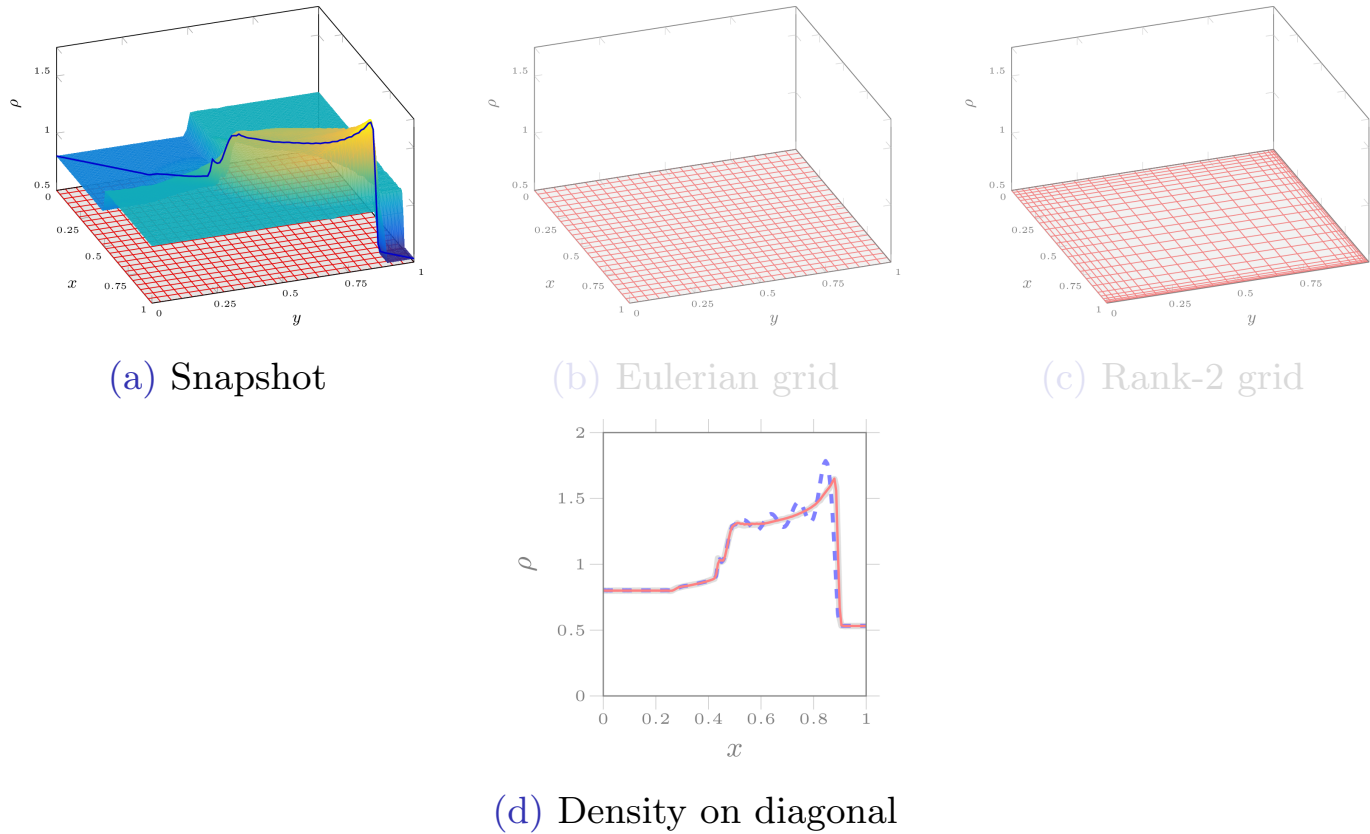


Figure 9: Density at $t = 0.25$

Two-dimensional Riemann problem

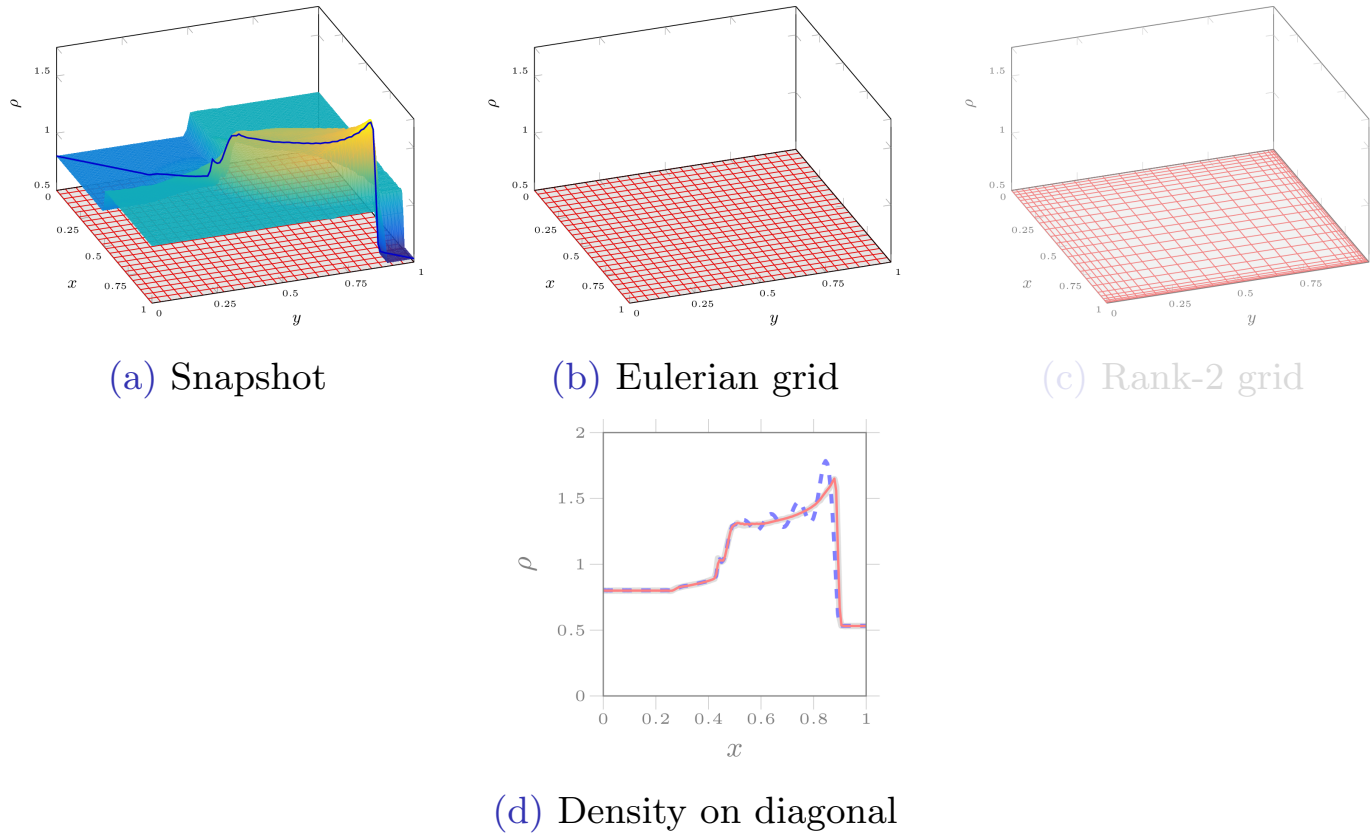
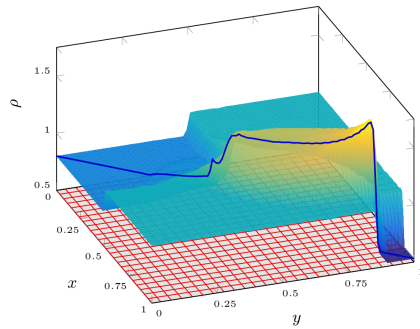
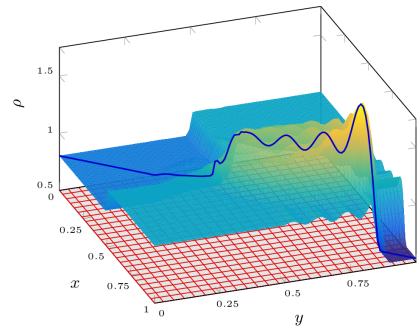
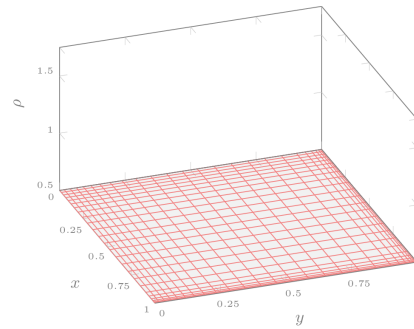


Figure 9: Density at $t = 0.25$

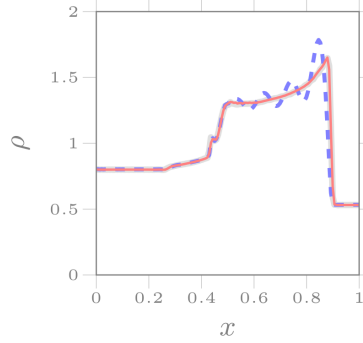
Two-dimensional Riemann problem



(a) Snapshot

(b) Eulerian grid, $k = 8$ 

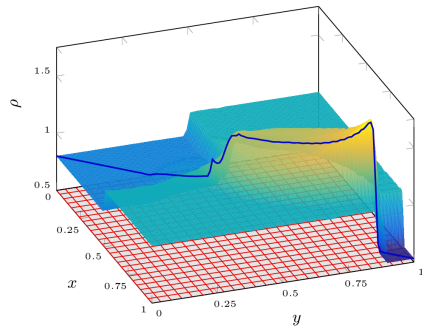
(c) Rank-2 grid



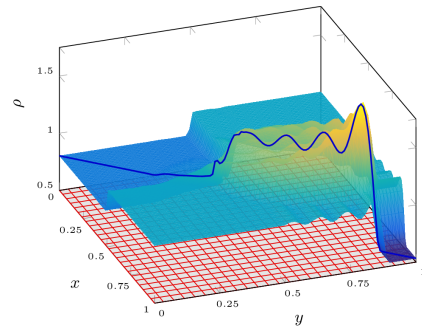
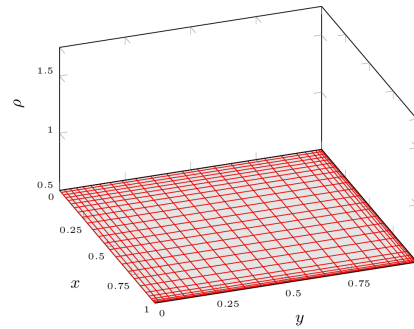
(d) Density on diagonal

Figure 9: Density at $t = 0.25$

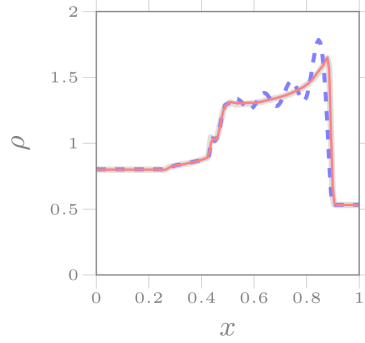
Two-dimensional Riemann problem



(a) Snapshot

(b) Eulerian grid, $k = 8$ 

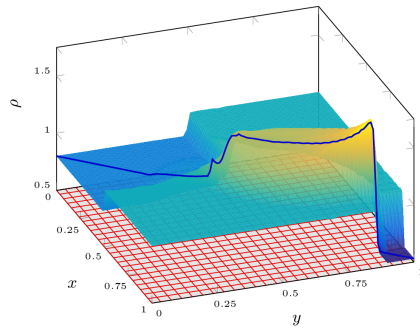
(c) Rank-2 grid



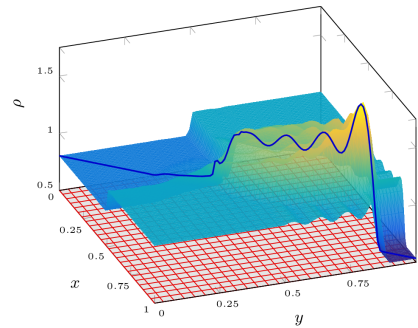
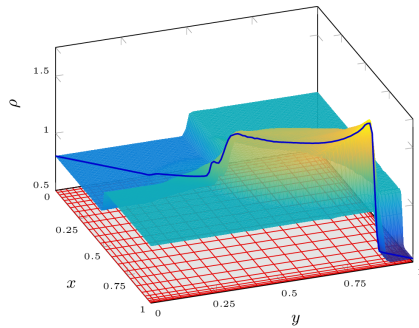
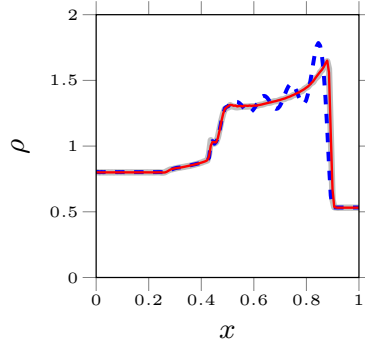
(d) Density on diagonal

Figure 9: Density at $t = 0.25$

Two-dimensional Riemann problem



(a) Snapshot

(b) Eulerian grid, $k = 8$ (c) Rank-2 grid, $k_r = 8$ 

(d) Density on diagonal

Figure 9: Density at $t = 0.25$

Two-dimensional Riemann problem

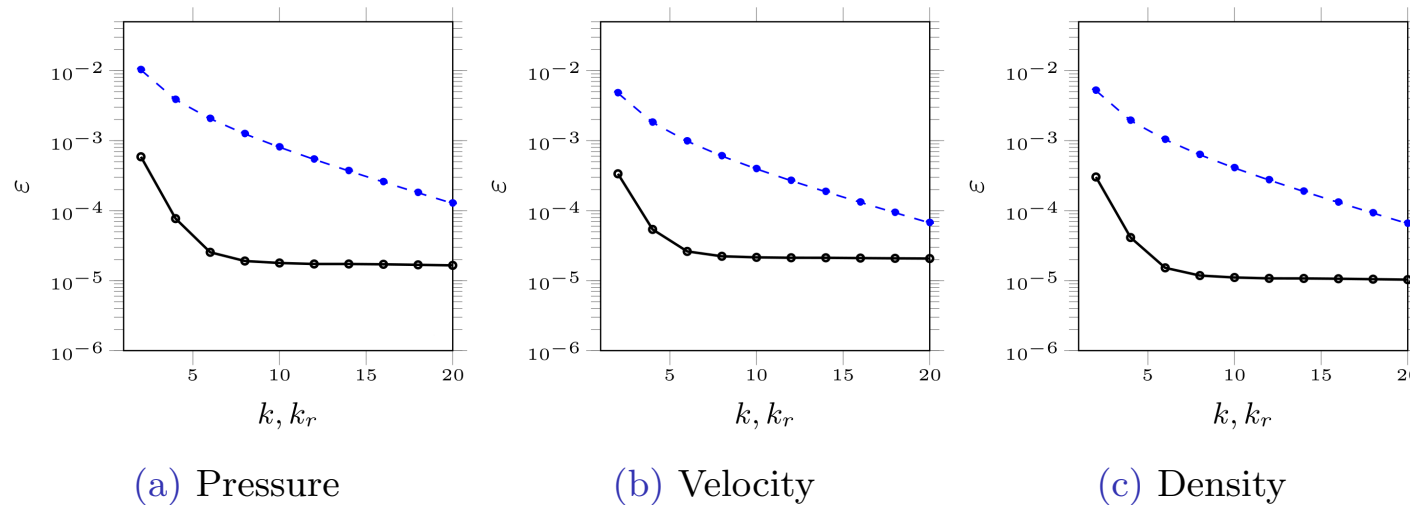


Figure 10: Reconstruction error. The rank- k reconstruction on POD subspace (dashed blue line), and rank- k_r reconstruction on the identified manifold of $r = 2$ (solid black line)

Summary

- Snapshots featuring convection cannot be efficiently compressed using traditional approaches
- A low-rank grid can be identified to efficiently compress/reduce such snapshots
- The proposed manifold approach *efficiently registers the output sequence of the PDEs on a low-rank time-varying grid*

Summary

- Snapshots featuring convection cannot be efficiently compressed using traditional approaches
- A low-rank grid can be identified to efficiently compress/reduce such snapshots
- The proposed manifold approach *efficiently registers the output sequence of the PDEs on a low-rank time-varying grid*

Summary

- Snapshots featuring convection cannot be efficiently compressed using traditional approaches
- A low-rank grid can be identified to efficiently compress/reduce such snapshots
- The proposed manifold approach *efficiently registers the output sequence of the PDEs on a low-rank time-varying grid*

Outline

1 Introduction

- Fundamentals
- Motivation

2 Identifying an optimal manifold

- Physics-aware registration-based manifold

3 ROMs on the identified manifold

- Projection based ROMs
- Neural Network based ROMs

4 Stabilization of time-varying ROMs

- A feedback controller approach

5 Summary

Constructing the ROMs

- Constructing the dynamical systems on the identified manifolds
 - Governing equations are available:
 - Projection-based reduced order models
 - Governing equations are *not* available:
 - System identification: Volterra series, Nonlinear Auto-Regressive Moving Average with eXogenous input (NARMAX), ...
 - Neural Networks: Recurrent Neural Networks (RNNs), ...

Constructing the ROMs

- Constructing the dynamical systems on the identified manifolds
 - Governing equations are available:
 - Projection-based reduced order models
 - Governing equations are *not* available:
 - System identification: Volterra series, Nonlinear Auto-Regressive Moving Average with eXogenous input (NARMAX), ...
 - Neural Networks: Recurrent Neural Networks (RNNs), ...

Step 1: identifying the POD subspace

- Given a snapshot matrix, $\mathbf{M} \in \mathbb{R}^{N \times K}$

$$\mathbf{M} = [\mathbf{w}_1 \quad \mathbf{w}_2 \quad \mathbf{w}_3 \quad \cdots \quad \mathbf{w}_K]; \quad \mathbf{w}_i \in \mathbb{R}^N \quad (14)$$

- The low-rank approximation problem is

$$\underset{\text{rank}(\widetilde{\mathbf{M}})=k}{\text{minimize}} \quad \|\mathbf{M} - \widetilde{\mathbf{M}}\|_F \quad (15)$$

- The rank constraint is satisfied

$$\underset{\mathbf{U} \in \mathbb{R}^{N \times k}, \mathbf{V} \in \mathbb{R}^{k \times K}}{\text{minimize}} \quad \|\mathbf{M} - \mathbf{UV}\|_F \quad (16)$$

- The solution is given by SVD/POD of the snapshot matrix

Step 1: identifying the POD subspace

- Given a snapshot matrix, $\mathbf{M} \in \mathbb{R}^{N \times K}$

$$\mathbf{M} = [\mathbf{w}_1 \quad \mathbf{w}_2 \quad \mathbf{w}_3 \quad \cdots \quad \mathbf{w}_K]; \quad \mathbf{w}_i \in \mathbb{R}^N \quad (14)$$

- The low-rank approximation problem is

$$\underset{\text{rank}(\widetilde{\mathbf{M}})=k}{\text{minimize}} \quad \|\mathbf{M} - \widetilde{\mathbf{M}}\|_F \quad (15)$$

- The rank constraint is satisfied

$$\underset{\mathbf{U} \in \mathbb{R}^{N \times k}, \mathbf{V} \in \mathbb{R}^{k \times K}}{\text{minimize}} \quad \|\mathbf{M} - \mathbf{UV}\|_F \quad (16)$$

- The solution is given by SVD/POD of the snapshot matrix

Step 1: identifying the POD subspace

- Given a snapshot matrix, $\mathbf{M} \in \mathbb{R}^{N \times K}$

$$\mathbf{M} = [\mathbf{w}_1 \quad \mathbf{w}_2 \quad \mathbf{w}_3 \quad \cdots \quad \mathbf{w}_K]; \quad \mathbf{w}_i \in \mathbb{R}^N \quad (14)$$

- The low-rank approximation problem is

$$\underset{\text{rank}(\widetilde{\mathbf{M}})=k}{\text{minimize}} \quad \|\mathbf{M} - \widetilde{\mathbf{M}}\|_F \quad (15)$$

- The rank constraint is satisfied

$$\underset{\mathbf{U} \in \mathbb{R}^{N \times k}, \mathbf{V} \in \mathbb{R}^{k \times K}}{\text{minimize}} \quad \|\mathbf{M} - \mathbf{UV}\|_F \quad (16)$$

- The solution is given by SVD/POD of the snapshot matrix

Step 1: identifying the POD subspace

- Given a snapshot matrix, $\mathbf{M} \in \mathbb{R}^{N \times K}$

$$\mathbf{M} = [\mathbf{w}_1 \quad \mathbf{w}_2 \quad \mathbf{w}_3 \quad \cdots \quad \mathbf{w}_K]; \quad \mathbf{w}_i \in \mathbb{R}^N \quad (14)$$

- The low-rank approximation problem is

$$\underset{\text{rank}(\widetilde{\mathbf{M}})=k}{\text{minimize}} \quad \|\mathbf{M} - \widetilde{\mathbf{M}}\|_F \quad (15)$$

- The rank constraint is satisfied

$$\underset{\mathbf{U} \in \mathbb{R}^{N \times k}, \mathbf{V} \in \mathbb{R}^{k \times K}}{\text{minimize}} \quad \|\mathbf{M} - \mathbf{UV}\|_F \quad (16)$$

- The solution is given by SVD/POD of the snapshot matrix

Step 2: constructing the reduced order model

- Consider the discretized system

$$\mathbf{R}(\mathbf{w}[n]) = \mathbf{0} \quad (17)$$

- The state, \mathbf{w} , is approximated on a global trial subspace,

$$\mathbf{w}[n] \approx \tilde{\mathbf{w}}[n] = \mathbf{U}\mathbf{w}_r[n], \quad \mathbf{U} \in \mathbb{R}^{N \times k}, \quad \mathbf{w}_r[n] \in \mathbb{R}^k, \quad k \ll N \quad (18)$$

- Galerkin projection onto the test subspace $\mathbf{U} \in \mathbb{R}^{N \times k}$,

$$\mathbf{U}^T \mathbf{R}(\mathbf{U}\mathbf{w}_r[n]) = \mathbf{0} \quad (19)$$

Step 2: constructing the reduced order model

- Consider the discretized system

$$\mathbf{R}(\mathbf{w}[n]) = \mathbf{0} \quad (17)$$

- The state, \mathbf{w} , is approximated on a global trial subspace,

$$\mathbf{w}[n] \approx \tilde{\mathbf{w}}[n] = \mathbf{U}\mathbf{w}_r[n], \quad \mathbf{U} \in \mathbb{R}^{N \times k}, \quad \mathbf{w}_r[n] \in \mathbb{R}^k, \quad k \ll N \quad (18)$$

- Galerkin projection onto the test subspace $\mathbf{U} \in \mathbb{R}^{N \times k}$,

$$\mathbf{U}^T \mathbf{R}(\mathbf{U}\mathbf{w}_r[n]) = \mathbf{0} \quad (19)$$

Step 2: constructing the reduced order model

- Consider the discretized system

$$\mathbf{R}(\mathbf{w}[n]) = \mathbf{0} \quad (17)$$

- The state, \mathbf{w} , is approximated on a global trial subspace,

$$\mathbf{w}[n] \approx \tilde{\mathbf{w}}[n] = \mathbf{U}\mathbf{w}_r[n], \quad \mathbf{U} \in \mathbb{R}^{N \times k}, \quad \mathbf{w}_r[n] \in \mathbb{R}^k, \quad k \ll N \quad (18)$$

- Galerkin projection onto the test subspace $\mathbf{U} \in \mathbb{R}^{N \times k}$,

$$\mathbf{U}^T \mathbf{R}(\mathbf{U}\mathbf{w}_r[n]) = \mathbf{0} \quad (19)$$

The proposed ROM

- Recall

$$\mathbf{w}[n] \approx \mathbf{U}\mathbf{w}_r[n] \quad (20)$$

- In the proposed new approach,

$$\mathbf{w}[n] \approx \mathbf{U}[n]\mathbf{w}_r[n] \quad (21)$$

where $\mathcal{G}^{-1}(\mathbf{U}) = \{\mathbf{U}[0], \mathbf{U}[1], \dots\}$

- For Galerkin ROM on the proposed manifold

$$\mathbf{U}^T[n]\mathbf{R}(\mathbf{U}[n]\mathbf{w}_r[n]) = \mathbf{0} \quad (22)$$

The proposed ROM

- Recall

$$\mathbf{w}[n] \approx \mathbf{U}\mathbf{w}_r[n] \quad (20)$$

- In the proposed new approach,

$$\mathbf{w}[n] \approx \mathbf{U}[n]\mathbf{w}_r[n] \quad (21)$$

where $\mathcal{G}^{-1}(\mathbf{U}) = \{\mathbf{U}[0], \mathbf{U}[1], \dots\}$

- For Galerkin ROM on the proposed manifold

$$\mathbf{U}^T[n]\mathbf{R}(\mathbf{U}[n]\mathbf{w}_r[n]) = \mathbf{0} \quad (22)$$

The proposed ROM

- Recall

$$\mathbf{w}[n] \approx \mathbf{U}\mathbf{w}_r[n] \quad (20)$$

- In the proposed new approach,

$$\mathbf{w}[n] \approx \mathbf{U}[n]\mathbf{w}_r[n] \quad (21)$$

where $\mathcal{G}^{-1}(\mathbf{U}) = \{\mathbf{U}[0], \mathbf{U}[1], \dots\}$

- For Galerkin ROM on the proposed manifold

$$\mathbf{U}^T[n]\mathbf{R}(\mathbf{U}[n]\mathbf{w}_r[n]) = \mathbf{0} \quad (22)$$

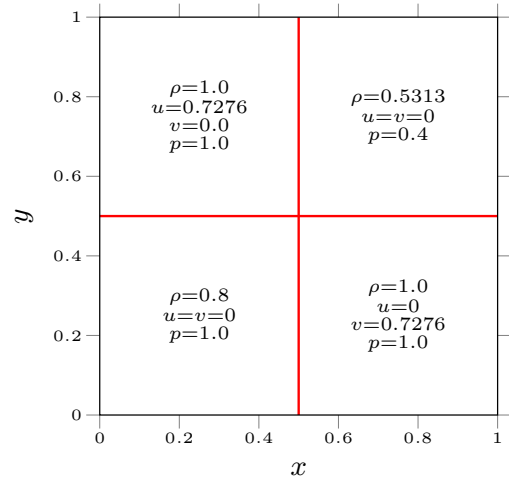
Numerical Example: Two-dimensional Riemann problem

- Consider the Euler equations

$$\left\{ \begin{array}{lcl} \frac{\partial}{\partial t} \mathbf{q} + \frac{\partial}{\partial x} \mathbf{f}_x + \frac{\partial}{\partial y} \mathbf{f}_y & = & 0, \quad (x, y, t) \in [0, 1] \times [0, 1] \times [0, t_{\max}] \\ \mathbf{q} & = & [\rho, \rho u, \rho v, \rho e]^T \\ \mathbf{f}_x & = & [\rho u, \rho u^2 + p, \rho uv, \rho uH]^T \\ \mathbf{f}_y & = & [\rho v, \rho uv + p, \rho v^2 + p, \rho vH]^T \\ H & = & e + p/\rho \\ p & = & \rho (\gamma - 1) (e - 0.5 (u^2 + v^2)) \end{array} \right. \quad (23)$$

- Stabilized using high-order artificial viscosity

Numerical Example: Two-dimensional Riemann problem



(a) Initial condition,
configuration 12
[Lax and Liu, 1998]

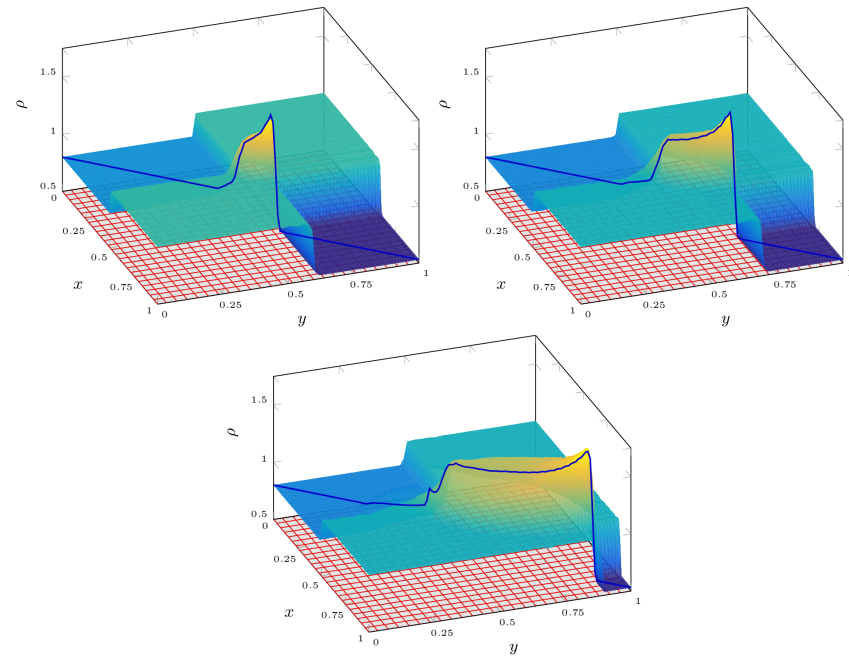
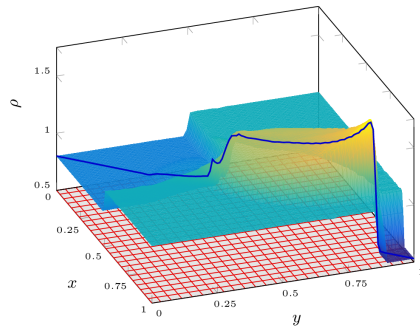
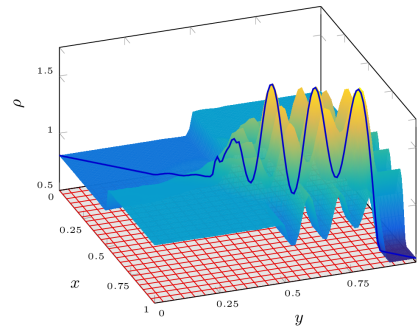
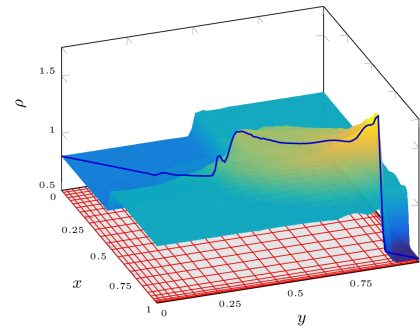
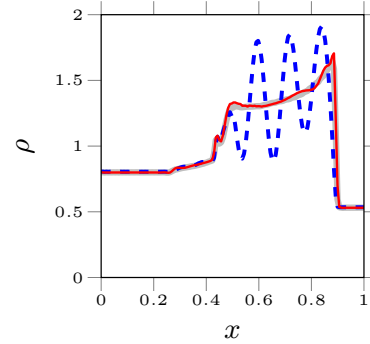


Figure 11: Two-dimensional Riemann problem

Numerical Example: Two-dimensional Riemann problem



(a) Snapshot

(b) Eulerian grid, $k = 8$ (c) Rank-2 grid, $k_r = 8$ 

(d) Density on diagonal

Figure 12: Density at $t = 0.25$

Numerical Example: Two-dimensional Riemann problem

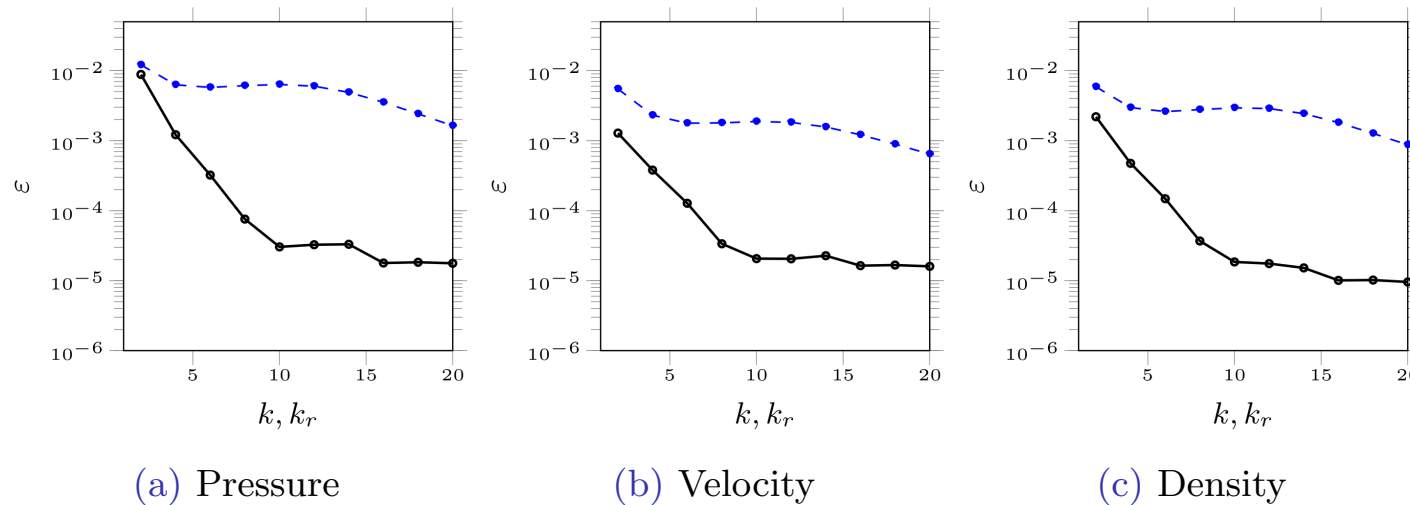
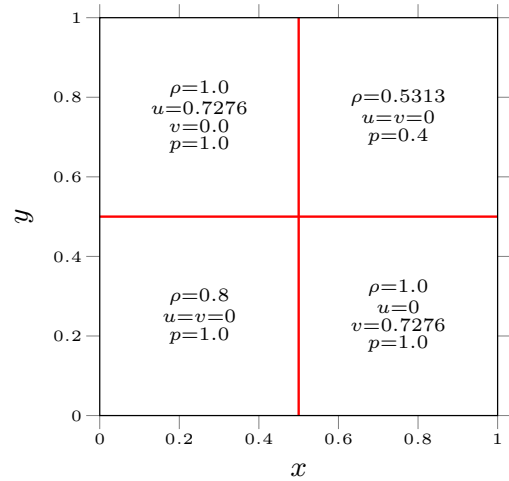


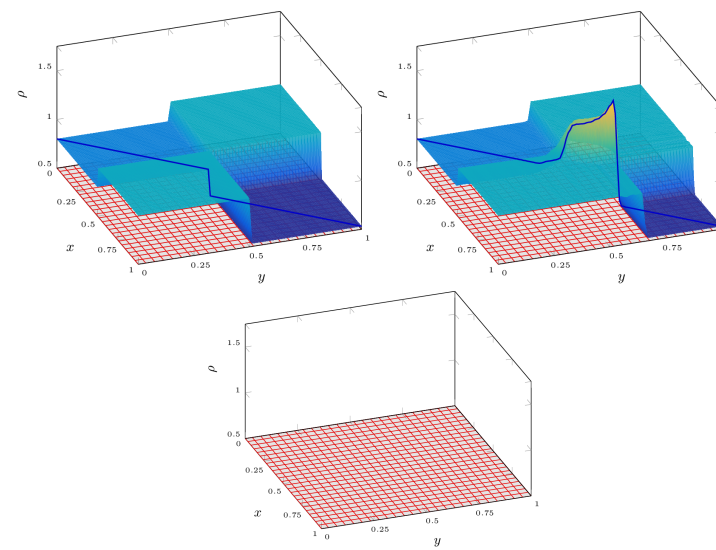
Figure 13: ROM error. The rank- k on POD subspace (dashed blue line), and rank- k_r on the identified rank-2 manifold (solid black line)

Numerical Example: Two-dimensional Riemann problem - Prediction

- The ROMs are evolved beyond the training range



(a) Initial condition,
configuration 12
[Lax and Liu, 1998]



(b) Density at $t \in \{0.0, 0.10\}$

Figure 14: Two-dimensional Riemann problem

Numerical Example: Two-dimensional Riemann problem - Prediction

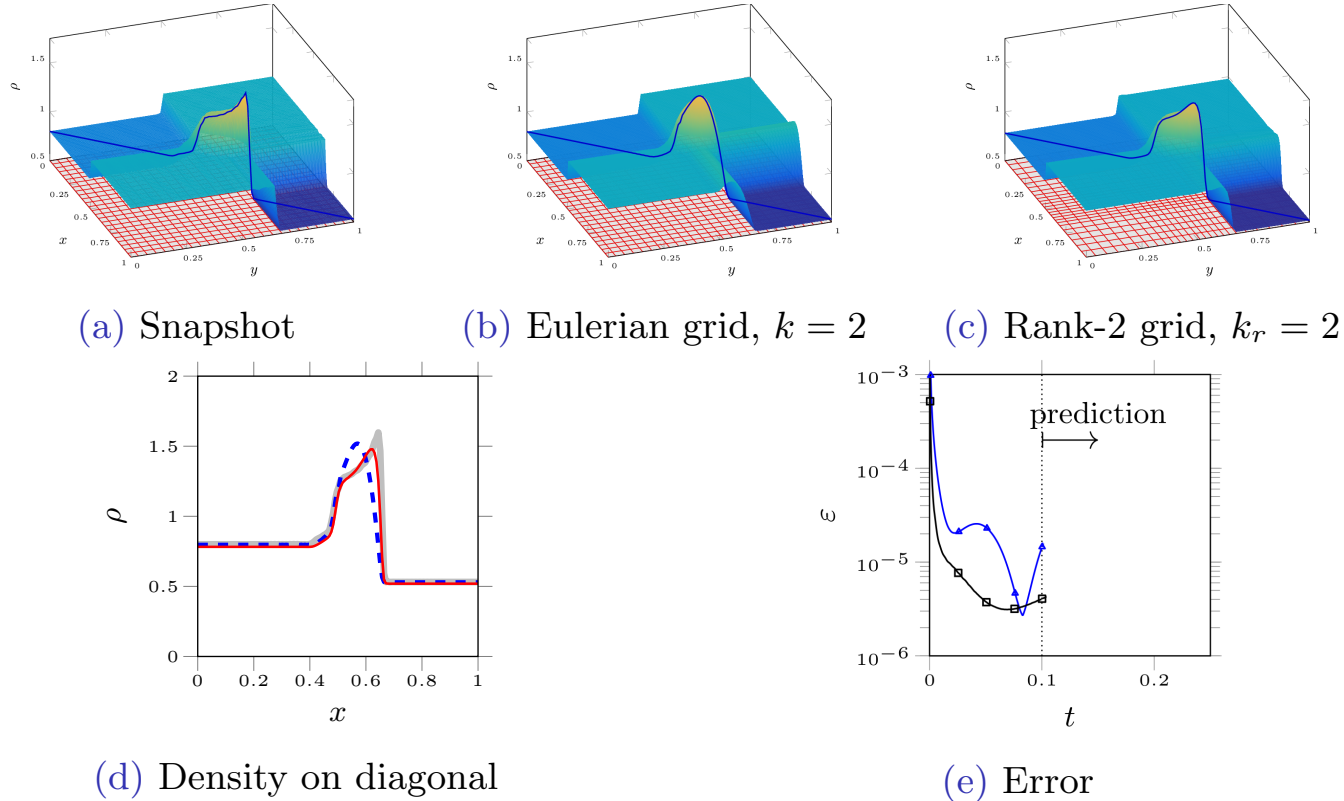


Figure 15: Density at $t = 0.1$, rank-2 ROM error on POD subspace (blue line) and rank-2 grid of the proposed manifold (black line)

Numerical Example: Two-dimensional Riemann problem - Prediction

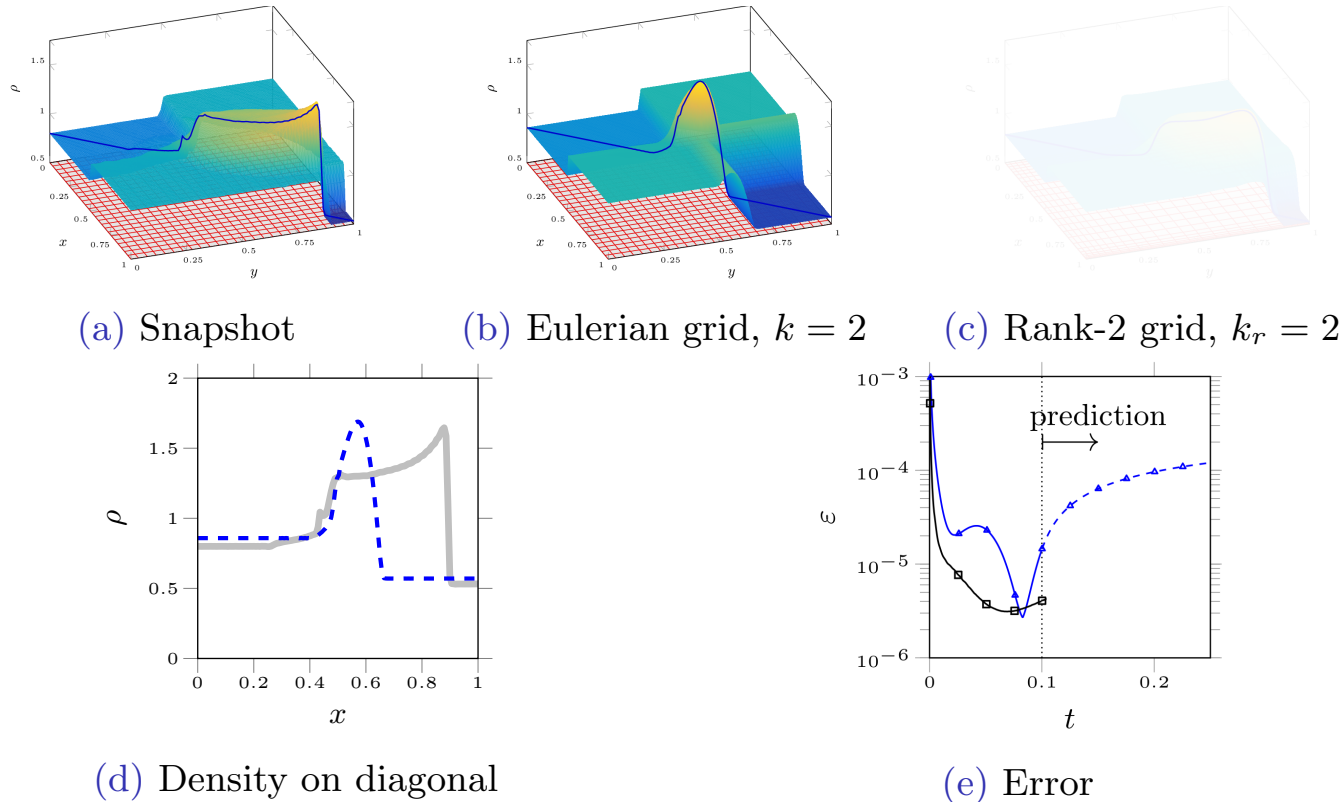


Figure 16: Density at $t = 0.25$, rank-2 ROM error on POD subspace (blue line) and rank-2 grid of the proposed manifold (black line)

Numerical Example: Two-dimensional Riemann problem - Prediction

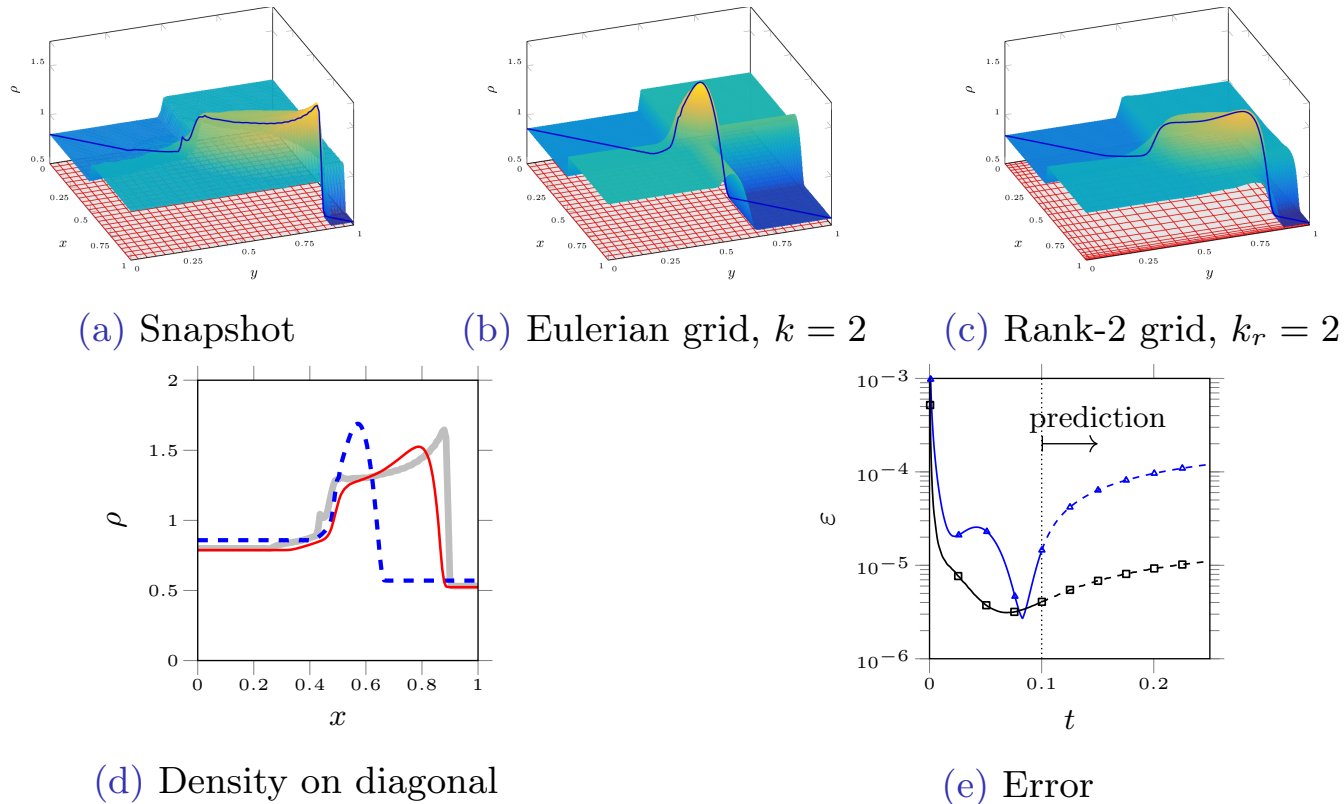


Figure 16: Density at $t = 0.25$, rank-2 ROM error on POD subspace (blue line) and rank-2 grid of the proposed manifold (black line)

Constructing the ROMs

- Constructing the dynamical systems on the identified manifolds
 - Governing equations are available:
 - Projection-based reduced order modeling
 - Governing equations are *not* available:
 - System identification: Volterra series, Nonlinear Auto-Regressive Moving Average with eXogenous input (NARMAX), ...
 - Neural Networks: [Recurrent Neural Networks \(RNNs\)](#), ...

Neural network-based ROMs

- Auto-encoders are trained to map to the low-dimensional space
- Recurrent neural networks (RNNs) are trained to approximate the dynamics on the low-dimensional space

$$\mathbf{h}[n] = f_{RNN}(\mathbf{h}[n-1]), \mathbf{h}[n] \in \mathbb{R}^k \quad (24)$$

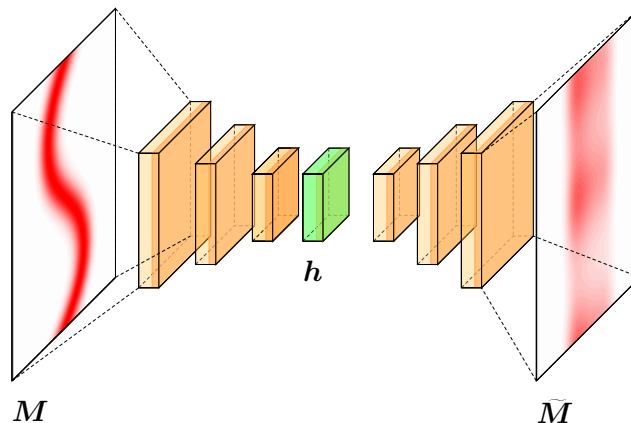


Figure 17: Neural network architecture with traditional auto-encoder

Neural network-based ROMs

- Auto-encoders are trained to map to the low-dimensional space
- Recurrent neural networks (RNNs) are trained to approximate the dynamics on the low-dimensional space

$$\boldsymbol{h}[n] = f_{RNN}(\boldsymbol{h}[n-1]), \boldsymbol{h}[n] \in \mathbb{R}^k \quad (24)$$

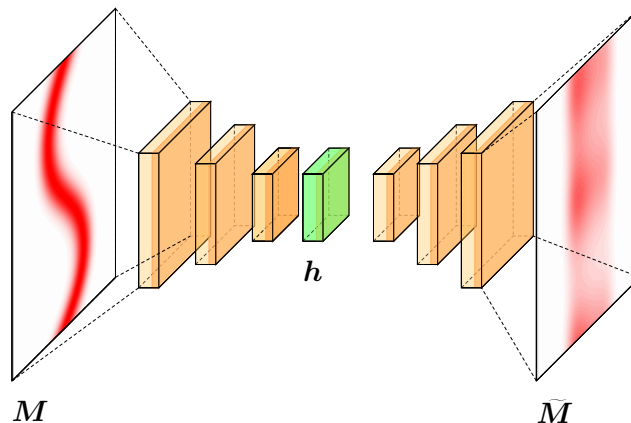


Figure 17: Neural network architecture with traditional auto-encoder

Neural network-based ROMs

- The traditional architecture is wrapped with the proposed manifold

$$\mathbf{h}[n] = f_{RNN}(\mathbf{h}[n-1]), \mathbf{h}[n] \in \mathbb{R}^{k_r} \quad (25)$$

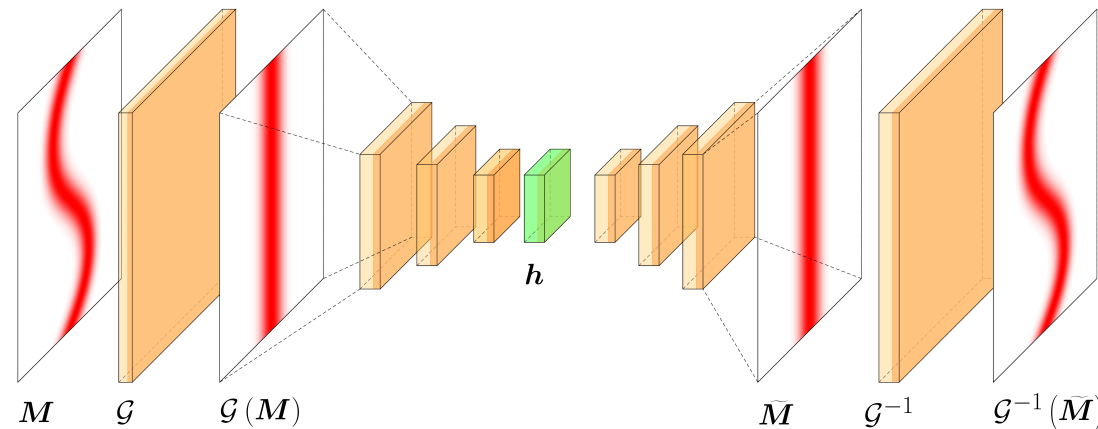


Figure 18: Neural network architecture with traditional auto-encoder wrapped with the proposed physics-aware auto-encoder

Numerical Example: Burgers' equation

- Consider the viscous Burgers' equation

$$\begin{cases} \frac{\partial w(x,t)}{\partial t} + w \frac{\partial w(x,t)}{\partial x} - 10^{-3} \frac{\partial^2 w(x,t)}{\partial x^2} = 0, & (x,t) \in [0, 2.5] \times [0, 1] \\ w(x,0) = 0.8 + 0.5e^{-(x-0.5)/0.1^2} \\ w(0,t) = 0.8 \\ w(2.5,t) = 0.8 \end{cases} \quad (26)$$

Numerical Example: Burgers' equation

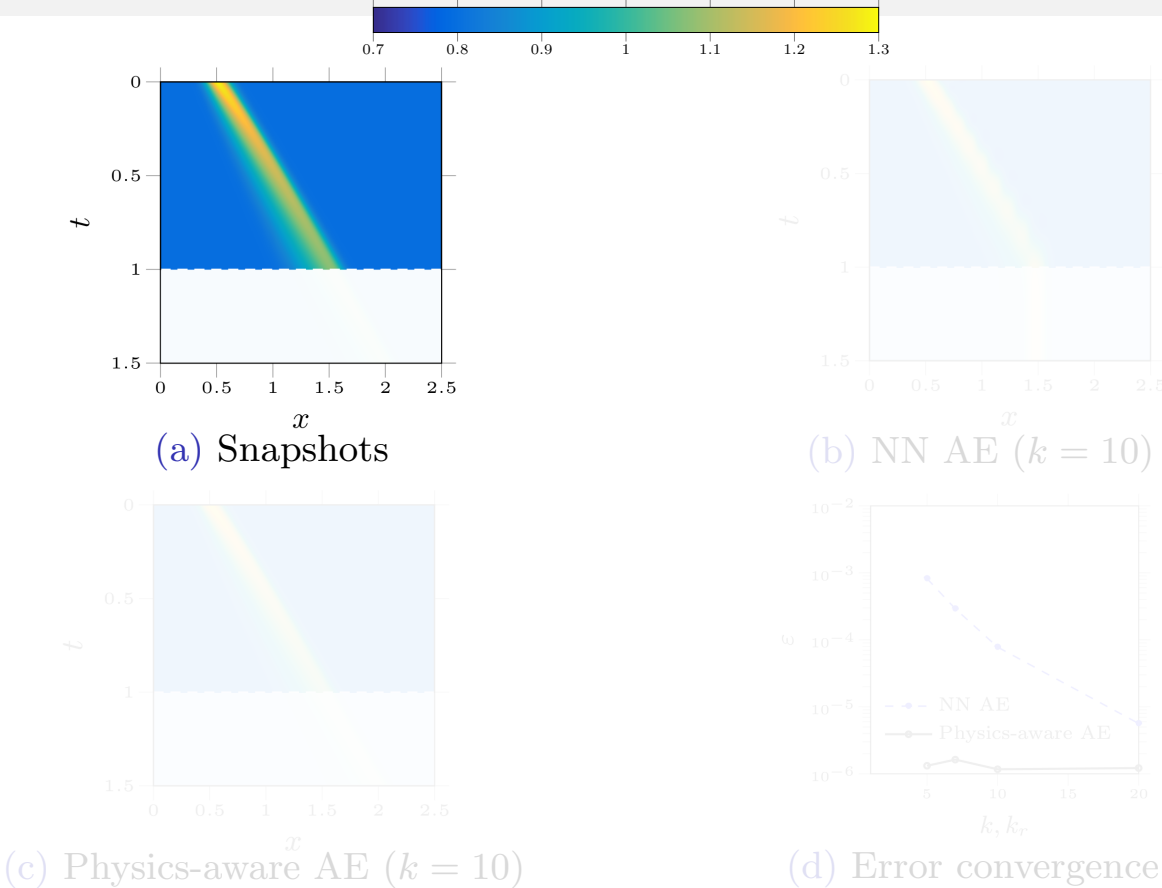


Figure 19: RNN for the Burgers' equation

Numerical Example: Burgers' equation

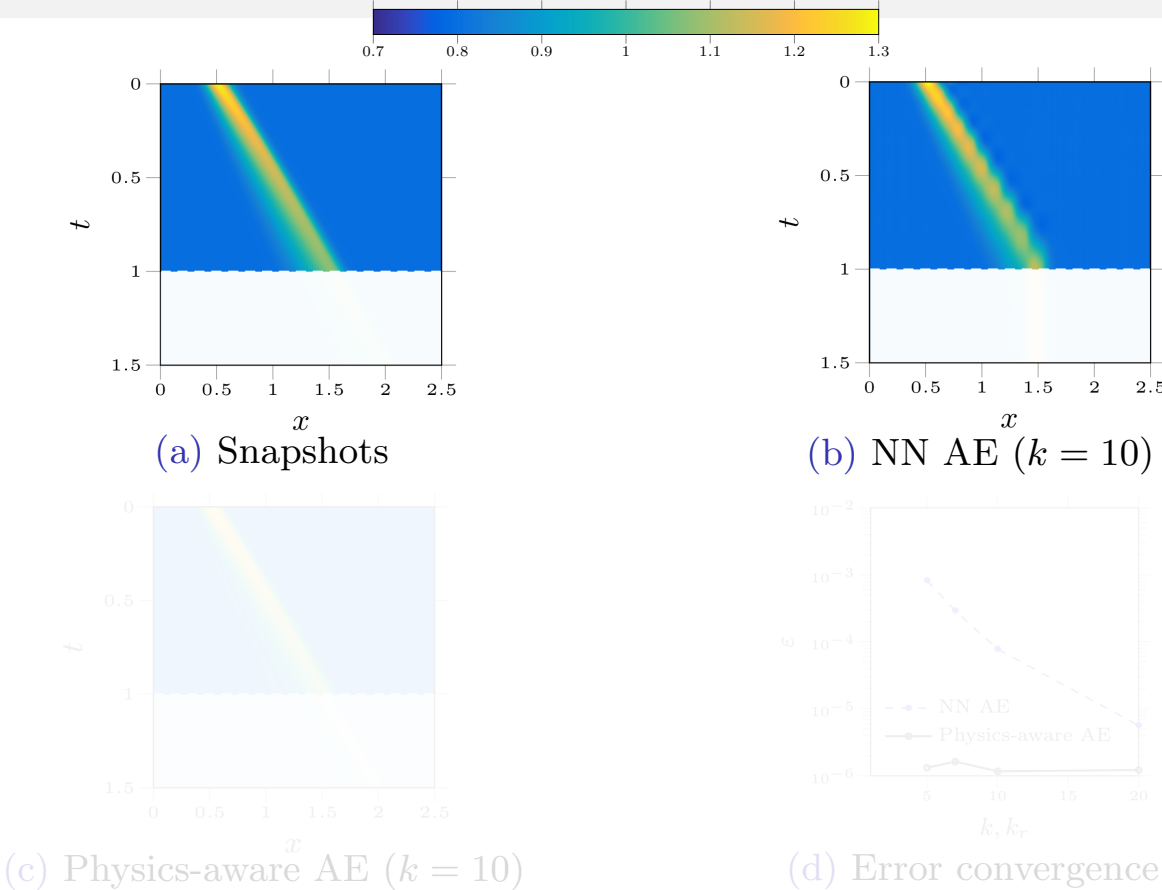


Figure 19: RNN for the Burgers' equation

Numerical Example: Burgers' equation

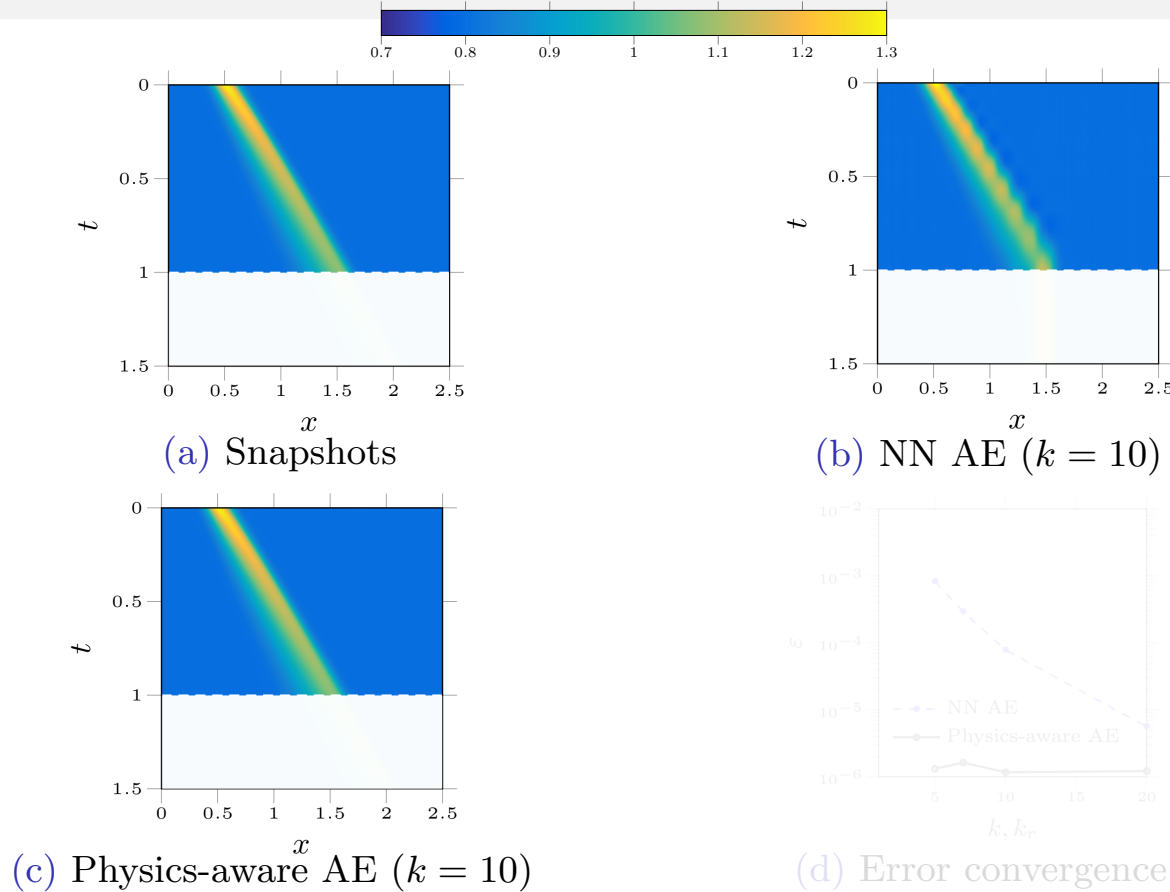


Figure 19: RNN for the Burgers' equation

Numerical Example: Burgers' equation

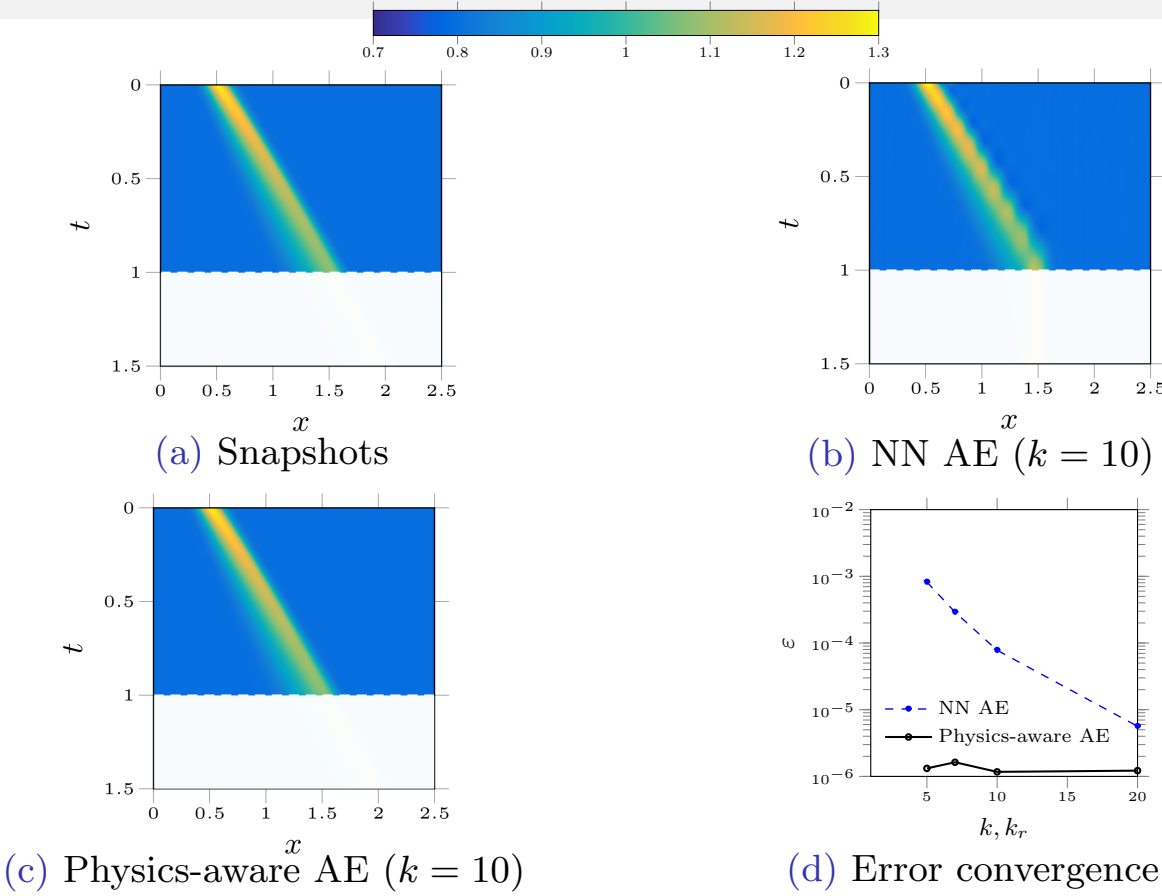


Figure 19: RNN for the Burgers' equation

Numerical Example: Burgers' equation

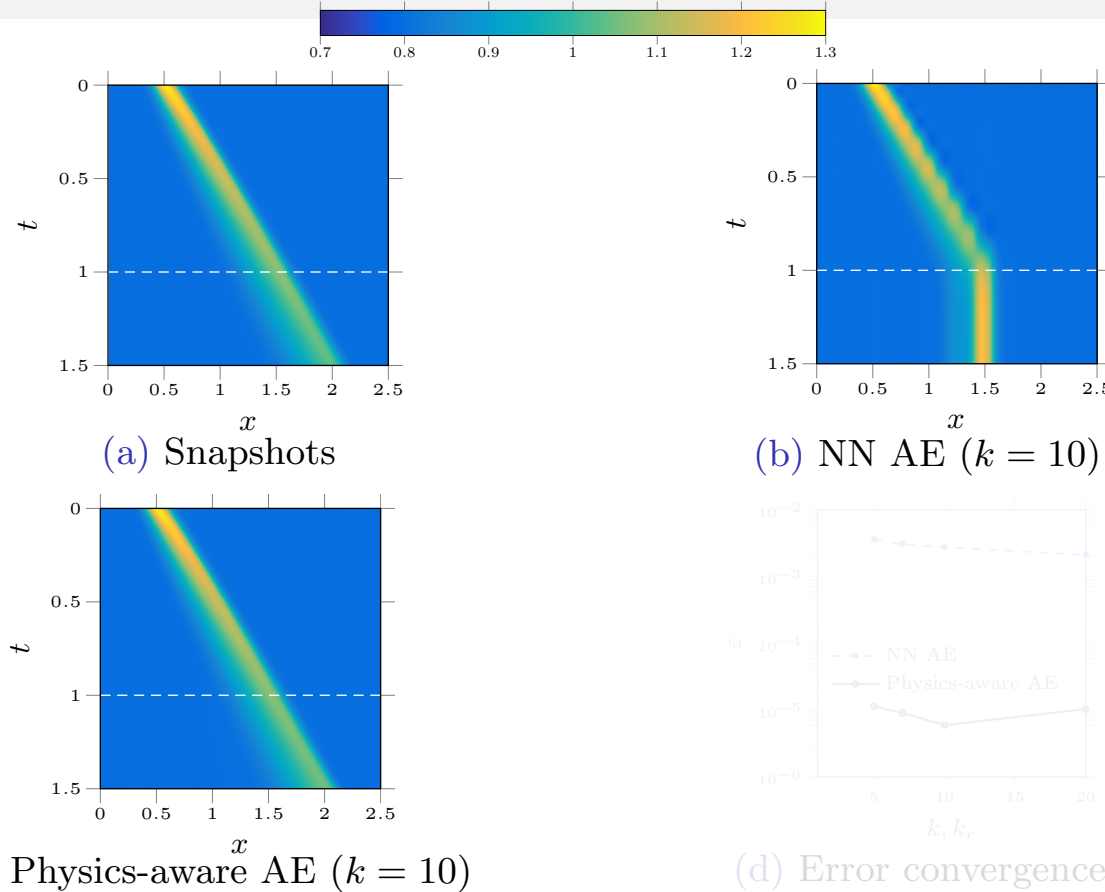


Figure 19: RNN for the Burgers' equation

Numerical Example: Burgers' equation

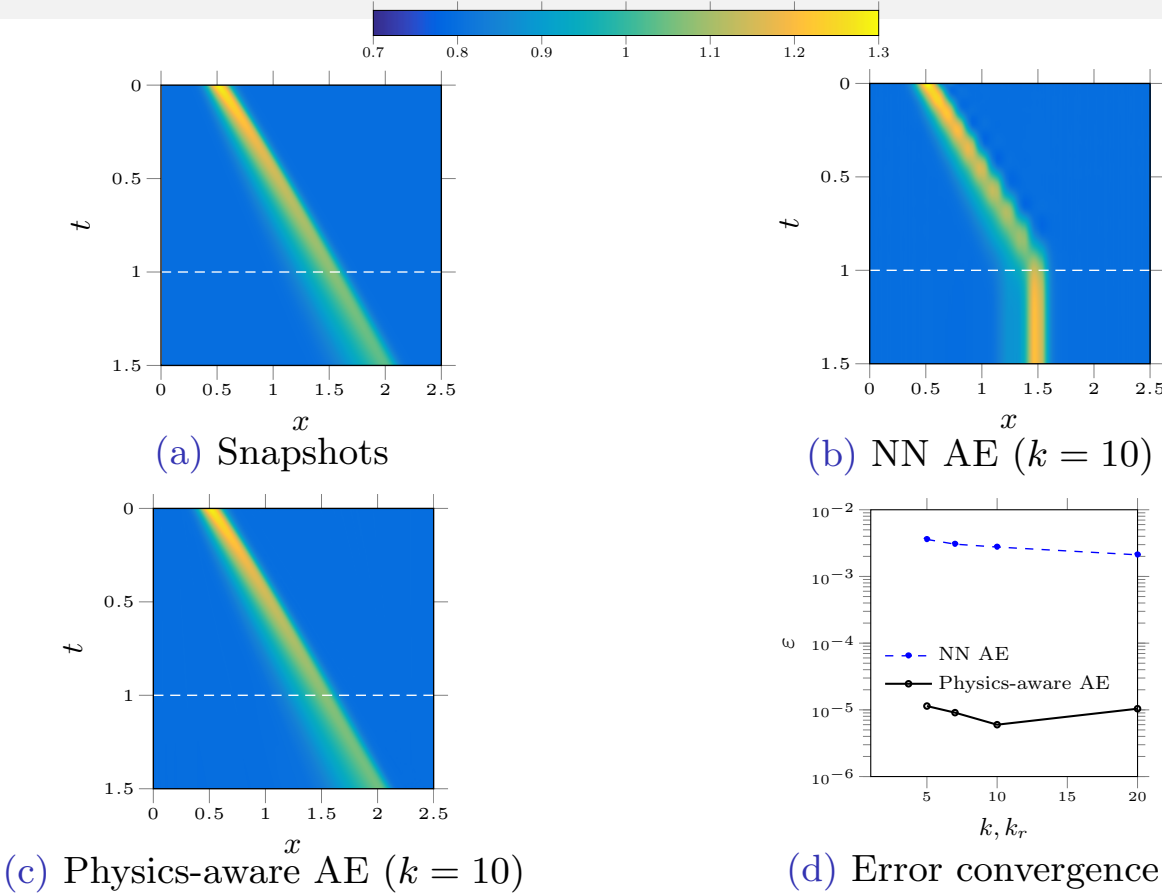


Figure 19: RNN for the Burgers' equation

Summary

- Non-intrusive ROMs on the proposed manifold can efficiently and accurately approximate the nonlinear convection dominated phenomena
- The proposed ROMs on the identified manifolds enable prediction
- Mojgani, R. and Balajewicz, M. “Projection based reduced order models on physics-aware registration based manifolds”, [under preparation].
- Mojgani, R. and Balajewicz, M. “Physics-aware registration based auto-encoder for convection dominated PDEs”, *AAAI 2021*, [under phase II review].
- Mojgani, R. and Balajewicz, M. “Dimensionality reduction of convection-dominated flows on an optimally morphing grid”, *APS Annual Meeting*, 2019.
- Mojgani, R. and Balajewicz, M. “Arbitrary Lagrangian Eulerian framework for efficient projection-based reduction of convection dominated nonlinear flows”, *APS Division of Fluid Dynamics Meeting*, 2017.
- Mojgani, R. and Balajewicz, M. “Lagrangian basis method for dimensionality reduction of convection dominated nonlinear flows”, *SIAM Conference on Computational Science and Engineering* 2017.
- Mojgani, R. and Balajewicz, M. “Lagrangian basis method for dimensionality reduction of convection dominated nonlinear flows”, *arXiv:1701.04343*.

Outline

1 Introduction

- Fundamentals
- Motivation

2 Identifying an optimal manifold

- Physics-aware registration-based manifold

3 ROMs on the identified manifold

- Projection based ROMs
- Neural Network based ROMs

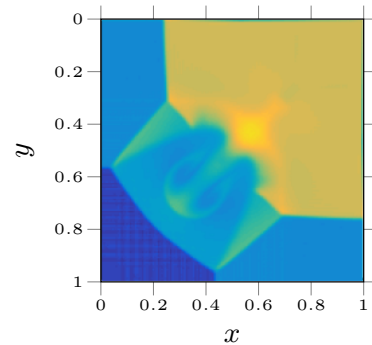
4 Stabilization of time-varying ROMs

- A feedback controller approach

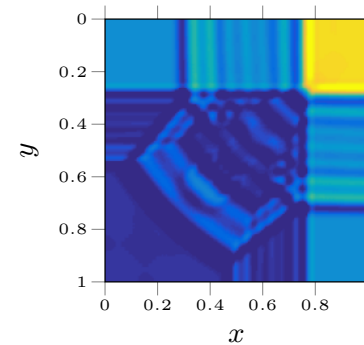
5 Summary

Stability of ROMs

- A projection-based ROM does not inherit the stability characteristics of the high fidelity model



(a) High fidelity model, $t = 0.80$



(b) ROM, $t = 0.15$

Figure 20: Two-dimensional Riemann problem, configuration 3 [Lax and Liu, 1998]

Stabilization of time-varying systems

- The stabilization problem

$$\begin{aligned}
 & \underset{\sigma_i[n]}{\text{minimize}} \quad \sum_{n=0}^{N_t} \|\mathbf{y}[n] - \hat{\mathbf{y}}_r[n]\|_2, \\
 & \text{subject to} \quad 1. \sigma_i^\Delta[n] \in \mathbb{R}^+, \text{ for } n \in \{0, \dots, N_t\}, \\
 & \quad 2. \sup_{n \geq n_0} \left\| \boldsymbol{\phi}_{\hat{\mathbf{A}}_r}[n, n_0] \right\|_2 \leq c[n_0],
 \end{aligned} \tag{27}$$

where $\sigma_i^\Delta[n]$ are change in the singular values of reduced system matrix

- Mojgani, R. and Balajewicz, M. "Stabilization of linear time-varying reduced order models, a feedback controller approach". *International Journal for Numerical Methods in Engineering*, [Accepted]

Outline

1 Introduction

- Fundamentals
- Motivation

2 Identifying an optimal manifold

- Physics-aware registration-based manifold

3 ROMs on the identified manifold

- Projection based ROMs
- Neural Network based ROMs

4 Stabilization of time-varying ROMs

- A feedback controller approach

5 Summary

Summary

- No reasonable low-rank approximation exists for solutions featuring moving interfaces, discontinuities, or sharp gradients
- An interpretable manifold learning approach successfully reduces the dimensionality of convection dominated flows
- The identified low-rank manifold enables ROMs with predictive capabilities
- The non-intrusive ROMs constructed on the identified manifolds are time-varying dynamical systems
- The time-varying ROMs can be stabilized by a feedback controller and their predictive capabilities are preserved

Summary

- No reasonable low-rank approximation exists for solutions featuring moving interfaces, discontinuities, or sharp gradients
- An interpretable manifold learning approach successfully reduces the dimensionality of convection dominated flows
- The identified low-rank manifold enables ROMs with predictive capabilities
- The non-intrusive ROMs constructed on the identified manifolds are time-varying dynamical systems
- The time-varying ROMs can be stabilized by a feedback controller and their predictive capabilities are preserved

Summary

- No reasonable low-rank approximation exists for solutions featuring moving interfaces, discontinuities, or sharp gradients
- An interpretable manifold learning approach successfully reduces the dimensionality of convection dominated flows
- The identified low-rank manifold enables ROMs with predictive capabilities
- The non-intrusive ROMs constructed on the identified manifolds are time-varying dynamical systems
- The time-varying ROMs can be stabilized by a feedback controller and their predictive capabilities are preserved

Summary

- No reasonable low-rank approximation exists for solutions featuring moving interfaces, discontinuities, or sharp gradients
- An interpretable manifold learning approach successfully reduces the dimensionality of convection dominated flows
- The identified low-rank manifold enables ROMs with predictive capabilities
- The non-intrusive ROMs constructed on the identified manifolds are time-varying dynamical systems
- The time-varying ROMs can be stabilized by a feedback controller and their predictive capabilities are preserved

Summary

- No reasonable low-rank approximation exists for solutions featuring moving interfaces, discontinuities, or sharp gradients
- An interpretable manifold learning approach successfully reduces the dimensionality of convection dominated flows
- The identified low-rank manifold enables ROMs with predictive capabilities
- The non-intrusive ROMs constructed on the identified manifolds are time-varying dynamical systems
- The time-varying ROMs can be stabilized by a feedback controller and their predictive capabilities are preserved

Summary

- No reasonable low-rank approximation exists for solutions featuring moving interfaces, discontinuities, or sharp gradients
- An interpretable manifold learning approach successfully reduces the dimensionality of convection dominated flows
- The identified low-rank manifold enables ROMs with predictive capabilities
- The non-intrusive ROMs constructed on the identified manifolds are time-varying dynamical systems
- The time-varying ROMs can be stabilized by a feedback controller and their predictive capabilities are preserved

This material is based upon work supported by

- Grainger College of Engineering, Computational Science and Engineering fellowship [2017-2018]
- The National Science Foundation under Grant No. CMMI-1435474
- The Air Force Office of Scientific Research under Grant No. FA9550-17-1-0203

Bibliography

-  Amsallem, D., Zahr, M. J., and Farhat, C. (2012).
Nonlinear model order reduction based on local reduced-order bases.
International Journal for Numerical Methods in Engineering, 92(10):891–916.
-  Babaee, H., Farazmand, M., Haller, G., and Sapsis, T. P. (2017).
Reduced-order description of transient instabilities and computation of finite-time Lyapunov exponents.
Chaos: An Interdisciplinary Journal of Nonlinear Science, 27(6):063103.
-  Carlberg, K. (2015).
Adaptive h-refinement for reduced-order models.
International Journal for Numerical Methods in Engineering, 102(5):1192–1210.
-  G.E, H. and R.R, S. (2006).
Reducing the dimensionality of data with neural networks.
Science, 313(July):504–507.
-  Gerbeau, J.-F. and Lombardi, D. (2014).
Approximated Lax pairs for the reduced order integration of nonlinear evolution equations.
Journal of Computational Physics, 265:246–269.
-  Iollo, A. and Lombardi, D. (2014).
Advection modes by optimal mass transfer.
Physical Review E, 89(2):022923.

Bibliography



Kavousanakis, M., Erban, R., Boudouvis, A. G., Gear, C. W., and Kevrekidis, I. G. (2007).
Projective and coarse projective integration for problems with continuous symmetries.
Journal of Computational Physics, 225(1):382–407.



Lax, P. D. and Liu, X.-d. (1998).
Solution of two-dimensional Riemann problems of gas dynamics by positive schemes.
SIAM Journal on Scientific Computing, 19(2):319–340.



Lu, H. and Tartakovsky, D. M. (2020).
Lagrangian dynamic mode decomposition for construction of reduced-order models of advection-dominated phenomena.
Journal of Computational Physics, 407:109229.



Lucia, D. J. (2001).
Reduced order modeling for high speed flows with moving shocks.
PhD thesis, Air Force Institute of Technology, Wright-Patterson Air Force Base, Ohio.



Maaten, L. v. d. and Hinton, G. (2008).
Visualizing data using t-SNE.
Journal of machine learning research, 9(November):2579–2605.



Mendible, A., Aravkin, A., Lowrie, W., Brunton, S., and J. Nathan Kutz (2019).
Dimensionality reduction and reduced order modeling for traveling wave physics.
arXiv preprint arXiv:1911.00565v1.

Bibliography



Mojgani, R. and Balajewicz, M. (2017).

Lagrangian basis method for dimensionality reduction of convection dominated nonlinear flows.
arXiv preprint arXiv:1701.04343.



Mowlavi, S. and Sapsis, T. P. (2018).

Model order reduction for stochastic dynamical systems with continuous symmetries.
SIAM Journal on Scientific Computing, 40(3):A1669–A1695.



Rapun, M.-L. and Vega, J. M. (2010).

Reduced-order models based on local POD plus Galerkin projection.
Journal of Computational Physics, 229(8):3046–3063.



Reiss, J., Schulze, P., and Sesterhenn, J. (2015).

The shifted proper orthogonal decomposition: A mode decomposition for multiple transport phenomena.
arXiv preprint arXiv:1512.01985.



Reiss, J., Schulze, P., Sesterhenn, J., and Mehrmann, V. (2018).

The shifted proper orthogonal decomposition: A mode decomposition for multiple transport phenomena.
SIAM Journal on Scientific Computing, 40(3):A1322–A1344.



Rim, D. and Mandli, K. T. (2018).

Model reduction of a parametrized scalar hyperbolic conservation law using displacement interpolation.
arXiv preprint arXiv:1805.05938v1.

Bibliography

-  Rim, D., Moe, S., and LeVeque, R. J. (2017).
Transport reversal for model reduction of hyperbolic partial differential equations.
arXiv preprint arXiv:1701.07529.
-  Rowley, C. W., Kevrekidis, I. G., Marsden, J. E., and Lust, K. (2003).
Reduction and reconstruction for self-similar dynamical systems.
Nonlinearity, 16(4):1257–1275.
-  Rowley, C. W. and Marsden, J. E. (2000).
Reconstruction equations and the Karhunen–Loève expansion for systems with symmetry.
Physica D: Nonlinear Phenomena, 142(1-2):1–19.
-  Schulze, P., Reiss, J., and Mehrmann, V. (2018).
Model reduction for a pulsed detonation combustor via shifted proper orthogonal decomposition.
arXiv preprint arXiv:1803.01805.
-  Taddei, T. (2020).
A registration method for model order reduction: Data compression and geometry reduction.
SIAM Journal on Scientific Computing, 42(2):A997–A1027.
-  Tenenbaum, J. B. (1998).
Mapping a manifold of perceptual observations.
In Jordan, M. I., Kearns, M. J., and Solla, S. A., editors, *Advances in Neural Information Processing Systems 10*, pages 682–688. MIT Press.